Chromosomal Imbalances and their Target Genes In Gastrointestinal Stromal Tumors

Reetta Ässämäki

Master's Thesis

University of Jyväskylä

Faculty of Mathematics and Science

Department of Biological and Environmental Science

Preface

University of Jyväskylä   **Abstract of Master's Thesis**
Faculty of Mathematics and Science

Abstract:

Gastrointestinal stromal tumor (GIST) is a mesenchymal sarcoma of the gastrointestinal tract. The tumors characteristically harbor *KIT* or *PDGFRA* mutations some of which are treatable with imatinib mesylate (Glivec^{TM}). However, the molecular and cytogenetic changes underlying the development and progression of GISTs are not fully understood. Chromosomal imbalances resulting in altered gene dosage are known to play a role in the molecular pathogenesis of these tumors but the target genes remain to be identified. The present study aimed to identify some of these genes. In total, 35 GIST samples were screened for chromosomal imbalances by array comparative genomic hybridization (array CGH). A cDNA-based array platform was used to define the minimal common overlapping areas of copy number change and the genes affected by them. Eight confirmative, replicate hybridizations were performed using an oligonucleotide-based array platform. Copy number losses were most recurrent at 14q, 22q, and 1p. Gains were less frequent overall with 8q being the most recurrent. Two recurrent copy number imbalances at 14q were recognized; 14q11.2 harboring *PARP2, APEX1* and *NDRG2* genes and 14q32.33 harboring *SIVA*. Additional proposed target genes identified were *NF2* at chromosome 22, *CDKN2A/2B* at 9p and *ENO1* at 1p for copy number losses and *KIT* at 4q, *MYC* at 8q and *MDM2* at 12q for copy number gains. Array CGH proved to be an effective tool for the identification of candidate genes involved in the development and progression of GISTs. Previously studied significant regions at 14q were further characterized and for the first time genes within these regions were directly identified. Furthermore, an important link that could explain both the loss of 1p and a gain of 8q frequently seen in the cytogenetic profile of GIST tumors was established between the loss of *ENO1* and a gain of *MYC*.

Keywords: Gastrointestinal stromal tumor, array comparative genomic hybridization, gene dosage, molecular pathogenesis

Jyväskylän Yliopisto   **Pro gradu -tutkielman tiivistelmä**
Matemaattis-luonnontieteellinen tiedekunta

Tekijä:	Reetta Ässämäki
Tutkielman nimi:	Kromosomaaliset muutokset ja niiden kohdegeenit gastrointestinaalisissa stromaalituumoreissa
English Title:	Chromosomal Imbalances and their Target Genes in Gastrointestinal Stromal Tumors
Päivämäärä:	31.5.2006 **Sivumäärä:** 72 + 10
Laitos:	Bio-ja ympäristötieteiden laitos
Oppiaine:	Molekyylibiologia
Tutkielman ohjaaja:	Sakari Knuutila

Tiivistelmä:

Gastrointestinaalinen stromaalituumori (GIST) on maha-suolikanavan mesenkyymin sarkooma, jossa luonteenomaisesti esiintyy aktivoiva mutaatio joko *KIT* tai *PDGFRA* geenissä. Osa GIST-tuumoreista on hoidettavissa imatinib mesylate (Glivec^{TM}) molekyylikohdennetulla lääkkeellä, kuitenkaan tuumorin kehittymisen ja etenemisen taustalla olevia molekyyli-ja sytogeneettisiä muutoksia ei vielä täysin ymmärretä. Tiedetään, että kromosomaaliset poikkeamat ja niiden aiheuttamat muutokset geeniannoksessa vaikuttavat GIST-tuumoreiden molekyylipatogenesiin mutta näiden poikkeamien kohdegeenit ovat vielä tunnistamatta. Tässä tutkimuksessa pyrittiin tunnistamaan joitakin näistä geeneistä. Kaiken kaikkiaan 35 GIST-näytteestä seulottiin kromosomaalisia muutoksia mikrosirupohjaisen vertailevan genomisen hybridisaation avulla. Pienimmät yhteiset päällekkäiset poikkeama-alueet ja niiden kohdegeenit identifioitiin komplimentaarisen DNA mikrosirun avulla. Kahdeksan varmentavaa toistohybridisaatiota tehtiin oligonukleotidi mikrosirua käyttäen. Geenin kopiomäärän häviämät olivat yleisimpiä lokaatioissa 14q, 22q ja 1p. Lisääntymät olivat pääpiirteisesti harvinaisempia kuin häviämät, toistuvin lisääntymä havaittiin lokaatiossa 8q. Kromosomista 14 löydettiin kaksi toistuvaa kromosomipoikkeamaa; 14q11.2 josta tunnistettiin geenit *PARP2, APEX1* ja *NDRG2* sekä 14q32.33 josta tunnistettiin geeni *SIVA*. Muita tutkimuksessa tunnistettuja ja kromosomimuutoksien kohdegeeneiksi esitettyjä geenejä ovat häviämissä *NF2* kromosomissa 22, *CDKN2A/2B* 9p:ssä ja *ENO1* 1p:ssä sekä lisääntymissä *KIT* 4q:ssa, *MYC* 8q:ssa ja *MDM2* 12q:ssa. Mikrosirupohjainen vertaileva genominen hybridisaatio osoittautui tehokkaaksi menetelmäksi GIST-tuumoreiden kehittymisen ja etenemisen kannalta tärkeiden kohdegeenien identifioimisessa. Lisäksi tutkimuksessa löydettiin tärkeä yhteys *ENO1* häviämän ja *MYC* lisääntymän välillä, tämä geenien välinen yhteys voi selittää sekä 1p:ssä usein havaitun häviämän että 8q:ssä havaitun lisääntymän. Kromosomissa 14 aeimmin havaitut poikkeama-alueet kyettiin tarkemmin määrittämään sekä ensimmäistä kertaa näiden poikkeamien kohdegeenit tunnistamaan.

Table of Contents

Abbreviations

ABL	v-abl Abelson murine leukemia viral oncogene homolog
aCGH	array CGH
APEX1	APEX nuclease (multifunctional DNA repair enzyme) 1
BAC	Bacterial Artificial Chromosome
BCR	Breakpoint cluster region
BSA	Bovine Serum Albumin
cCGH	chromosomal/conventional CGH
CDKN2A	cyclin-dependent kinase inhibitor 2A (melanoma, p16, inhibits CDK4)
CDKN2B	cyclin-dependent kinase inhibitor 2B (p15, inhibits CDK4)
cDNA	Complimentary DNA
CGH	Comparative Genomic Hybridization
CML	Chronic Myeloid Leukemia
CSF-1	Colony-stimulating factor-1
DNA	Deoxyribonucleic acid
ENO1	enolase 1, (alpha)
ERBB2	v-erb-b2 erythroblastic leukemia viral oncogene homolog
EST	Expressed Sequence Tag
FISH	Fluorescent in situ hybridization
FOS	v-fos FBJ murine osteosarcoma viral oncogene homolog
G-band	Giemsa banding
GIST	Gastrointestinal Stromal Tumor
GI-tract	Gastrointestinal tract
HE staining	Hematocyclin and eosin staining
HPF	High power field
IAA	Isoamyl alcohol
IIC	Intestinal cells of Cajal
KIT	v-kit Hardy-Zuckerman 4 feline sarcoma viral oncogene homolog
LOH	Loss of heterozygosity analysis
MDM2	Mdm2, transformed 3T3 cell double minute 2, p53 binding protein
MYC	v-myc myelocytomatosis viral oncogene homolog (avian)
NDRG2	NDRG family member 2
NF2	neurofibromin 2 (bilateral acoustic neuroma)
PAC	P1-derived artificial chromosome (Based on bacteriophage P1 genome)
PARP2	Poly (ADP-ribose) polymerase family, member 2
PCR	Polymerase chain reaction
PDGFRA	Platelet derived growth factor alpha
RNA	Ribonucleic acid
SCF	Stem cell factor
SDS	Sodium Dodecyl Sulfate
SIVA	CD27-binding (Siva) protein

1. Introduction

This thesis work is done in the field of cytomolecular genetics. The introduction aims to explain what cytogenetics is and how it is related to cancer research. Secondly the research method used in this study, namely comparative genomic hybridization will be explained in detail. Next the research subject; gastrointestinal stromal tumor will be described and both the history and current knowledge on the research of this tumor will be elucidated. Throughout the introduction emphasis is put on the diagnosis, prognosis and treatment of gastrointestinal stromal tumors. Finally in the results and discussion the results of a screening study of 35 gastrointestinal stromal tumors will be represented and discussed in the light of previous research.

1.1 Cytogenetics and the Genetics of Cancer

Cytogenetics is a study of human chromosomes. It comprises routine analysis of G-banded chromosomes, other cytogenetic banding techniques, as well as molecular cytogenetics such as fluorescent in situ hybridization (FISH), loss of heterozygosity analysis (LOH) and comparative genomic hybridization (CGH). Chromosomal abnormalities are known to cause certain human disorders such as Down syndrome and Fragile X syndrome; they are also responsible for at least half of spontaneous abortions. In addition to these germ line abnormalities chromosomal abnormalities in somatic cells underlie the formation of many cancers.

The basis of cytogenetics and cancer cytogenetics was laid by techniques that allowed examination of chromosomes in lymphocytes of peripheral blood. Preparations of metaphase chromosomes also called metaphase spreads are made so that a drop of anticoagulated peripheral blood is applied to tissue culture medium. Phytohemagglutinin is added to agglutinate the red blood cells and stimulate lymphocytes to divide and colchicine is added to block mitosis so that the chromosomes are left as they are in the metaphase of mitosis. Next

the cells are lysed and the metaphase chromosomes are stained for microscopic viewing. The most widely used staining technique is Giemsa banding (G-banding). It is performed by first adding trypsin to the chromosome preparations followed by adding of Giemsa stain. The pattern that is produced stains each chromosome with light and dark bands of unique organization and allows the identification of all human chromosomes as well as the detection of possible abnormalities. The dark bands of G-banding contain A-T rich DNA whereas light bands represent G-C rich DNA. Different resolutions of G-banding can be achieved by advanced techniques of chromosome preparations which allow the blocking of mitosis in different sub stages of metaphase. Ideograms of normal human chromosomes can be obtained at 400-band, 550-band and 850-band resolution per haploid set. The bands are numbered starting from the centromere and moving towards the chromosome arms. The centromere divides all chromosomes into two arms which by convention are called the p- (for petite) and q-arm so that p-arm represents the shorter chromosome arm and q-arm the longer arm. Figure 1 shows a G-banded ideogram of human chromosome 14 with three different resolutions.
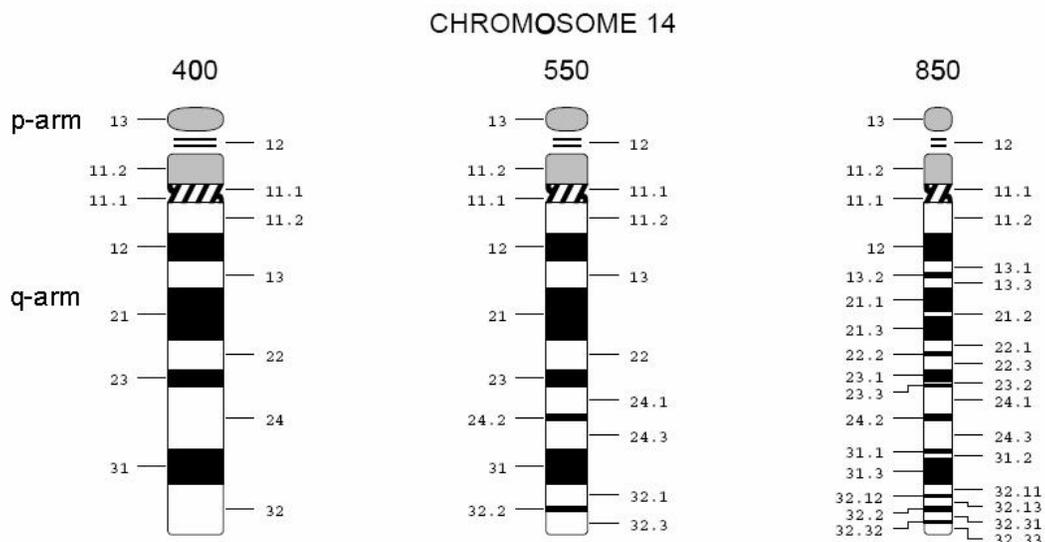

FIGURE 1. G-banded ideogram of human chromosome 14 displaying the three different resolutions of banding pattern. (http://www.pathology.washington.edu/research/cytopages/)

Human chromosomes display different morphology so that metacentric chromosomes have centromere in the middle of chromosome, submetacentric chromosomes have centromere

located somewhat towards the end of chromosome and acrocentric chromosomes such as that in Figure 2 have the centromere near the end of chromosome. Human chromosomes 13,14,15,21 and 22 are acrocentric and the short arm of these chromosomes forms a stalk like appendage called a satellite. The DNA in a satellite contains multiple repeated copies of ribosomal RNA genes. In the human karyotype of G-banded chromosomes the chromosomes are placed in groups according to their size and morphology. The difference between human karyotype of a metaphase spread and an ideogram of human karyotype is that in the former the sister chromatids are so adjacent that they appear as a single structure whereas in the latter the chromosomes are schematically X-shaped as seen in Figure 2.
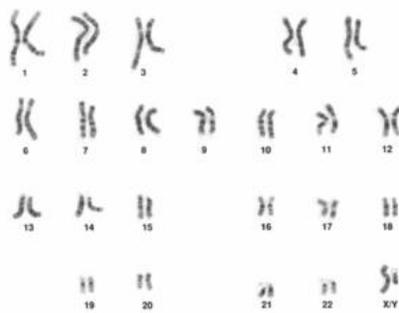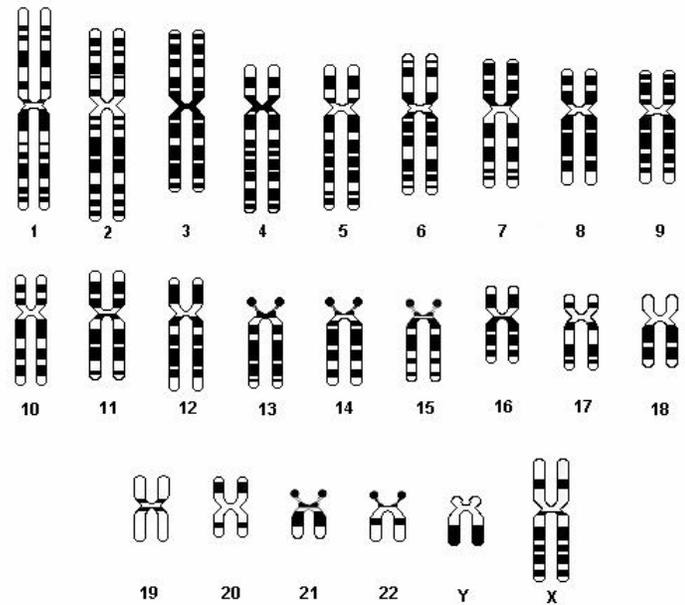
FIGURE 2. Human karyotype prepared from a metaphase spread (A) and displayed as a schematic ideogram (B). (http://en.wikipedia.org/wiki/Karyotype; http://wsrv.clas.virginia.edu/~rjh9u/ideo.html)

Chromosomal abnormalities are generally divided into numerical and structural abnormalities. Numerical abnormalities refer to ploidy which can be defined trough euploidy. Euploid is any precise multiple of N when N refers to the number of chromosomes in a normal haploid gamete. Aneuploid chromosome number is then any number of chromosomes that is not euploid and differs from normal diploid (2N) human karyotype 46, XX or 46, XY. Typical aneuploid karyotypes have either monosomies such as 45, X (Turner syndrome) or trisomies

such as 47, XY, +21 (a male with Down syndrome). Structural chromosomal abnormalities can involve either one or two chromosomes resulting in to deletions, duplications or inversion in the former and to insertions and translocations in the latter. Translocations can be further divided into reciprocal translocations and Robertsonian translocations, the latter lead to the loss of short arms and fusion of long arms of the acrocentric chromosomes. Translocation is an exchange of genetic material between nonhomologuos chromosomes and the effect of translocation depends on the breakage and reunion of exchanced material. If no genetic material is lost and no genes are damaged in the event of translocation the translocation is balanced and there is no clinical outcome for the individual however in the reverse case the translocation is unbalanced and can have clinical consequences.

Fluorescent in situ hybridization (FISH) is a method that can be used to detect chromosomal abnormalities in birth defects and cancer; it effectively combines conventional cytogenetics and molecular genetics. The advantage of FISH over conventional cytogenetic methods is that in addition to metaphase spreads it can be used also for cells in interphase. The technique uses specific DNA probes which are labeled with fluorochromes and applied on the patient sample where the DNA probe hybridizes to its target sequence. After hybridization the result is visualized using a fluorescent microscope. Depending on the type of probe used different chromosomal abnormalities can be detected. Centromeric probes hybridize to the centromeric region of specific chromosomes and can be used to detect numerical chromosomal abnormalities such as Down syndrome. Chromosome specific unique sequence probes can be designed for deletions that are known to cause certain diseases, whole chromosome paint probes are used to identify chromosomal rearrangements such as translocations and telomeric probes can be used to study subtelomeric abnormalities. Figure 3 demonstrates the application of FISH.
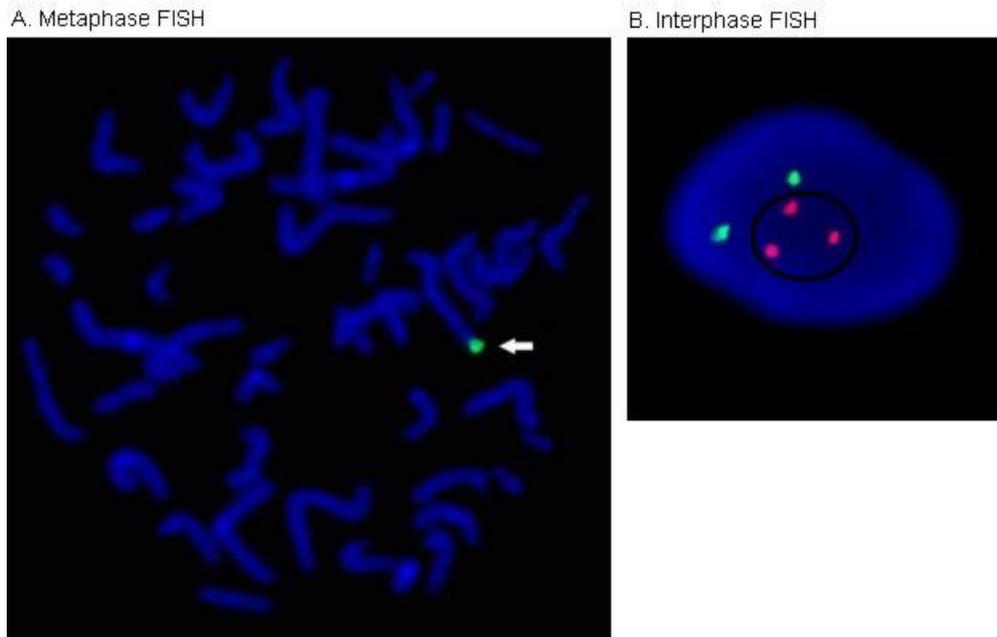
FIGURE 3. A) Metaphase FISH hybridized with terminal 4q probe. There is only one signal for the probe indicating that the other chromosome pair is lacking material from the terminal part of q-arm. B) Interphase FISH hybridized with two probes, one for chromosome 21 (circled) and another for chromosome 13. There are three signals for chromosome 21 indicating trisomy 21 i.e. Down syndrome. (http://members.aol.com/chrominfo/fishinfo.htm)

Chromosomal abnormalities can take place either in the germline causing genetic diseases and birth defects or in somatic cells in which case they can be related to certain types of cancer. Because specific and consistent chromosomal abnormalities are seen in many leukemias and solid tumors the investigation of chromosomal abnormalities is an important tool in cancer diagnostics and prognosis. The genetics of cancer is closely related to oncogenes and tumor suppressor genes. Oncogenes were originally identified from acute transforming retroviruses which produced tumors through transforming genes carried by the virus. Since then many oncogenes have also been identified from chromosomal translocation breakpoints or at amplified chromosomal regions. Oncogenes are activated, altered forms of corresponding normal cellular genes called proto-oncogenes. Oncogenes are involved in the various pathways of cell growth and differentiation. The three main methods of oncogene activation are point mutations, amplifications and translocations. Point mutations can change proto-oncogenes so that they became activated oncogenes whereas an amplification or gain of gene copy number can lead to malignant overexpression of the protein product. Translocations can activate proto-oncogenes by transferring them under a strong promoter of some other gene

or by a creation of chimeric fusion gene with malignant potential. Tumor suppressor genes on the other hand are genes involved in the control of cell proliferation. First identified in the research of malignant childhood cancer of the eye the retinoblastoma tumor suppressors usually require deletion of both alleles in order to be inactivated. This so called two hit model explains why an individual may have a genetic predisposition to cancer. A person may have inherited one nonfunctional allele of a tumor suppressor gene and thus only has one functional allele in all cells of the individual. One additional inactivating alteration directed to this functional allele in any cell of the individual will thus lead to loss of function of the particular tumor suppressor. The incidence that two such alterations occur in a same cell of a normal individual is much more unlikely. In addition to a loss of function mutation a person may have a loss of heterozygosity (LOH) or a loss of gene copy number in a tumor suppressor gene. Loss of heterozygosity means that instead of having one allele inherited from the mother and one allele inherited from the father the tumor cells are homozygous for a given tumor suppressor displaying a loss of one of the alleles. LOH can occur through a deletion of one chromosome pair, a deletion of chromosomal material comprising the allele or a cross over between two nonfunctional alleles which lead to homozygosity of mutant alleles. LOH has been identified in a number of cancers including the retinoplastoma and LOH analysis are therefore widely used in cancer research to identify potential locations for tumor suppressor genes. LOH is detected by PCR analysis of polymorphic alleles located in the introns or flanking regions of selected gene. The selected polymorphic microsatelite DNA markers in normal and tumor cells are compared and LOH is recognized where normal cell displays two alleles and tumor cell only one.

1.1.1 Comparative Genomic Hybridization

In addition to LOH analysis DNA copy number alteration can be studied by conventional, chromosomal comparative genomic hybridization or by genomic microarrays. The advantage of comparative genomic hybridization over LOH is that it has a potential to identify both oncogenes and tumor suppressor genes. The original method of comparative genomic hybridization (CGH) was developed by Kallioniemi et al. in 1992 (Kallioniemi et al.,

1992). They used normal metaphase spreads as a probe for fluorochrome labeled test and reference DNA. As a result of competitive hybridization to the chromosomes a relative copy number change based on the physical chromosomal location of DNA could be determined. The two fluorochrome intensities as well as their ratio were measured and a map of DNA sequence copy number as a function of chromosomal location was generated. The copy number profile represented the entire genome however the map was based on physical chromosomal map only and provided a resolution of approximately 10Mb. Figure 4 shows a typical chromosomal CGH copy number profile.

Copy number profile from chromosomal CGH
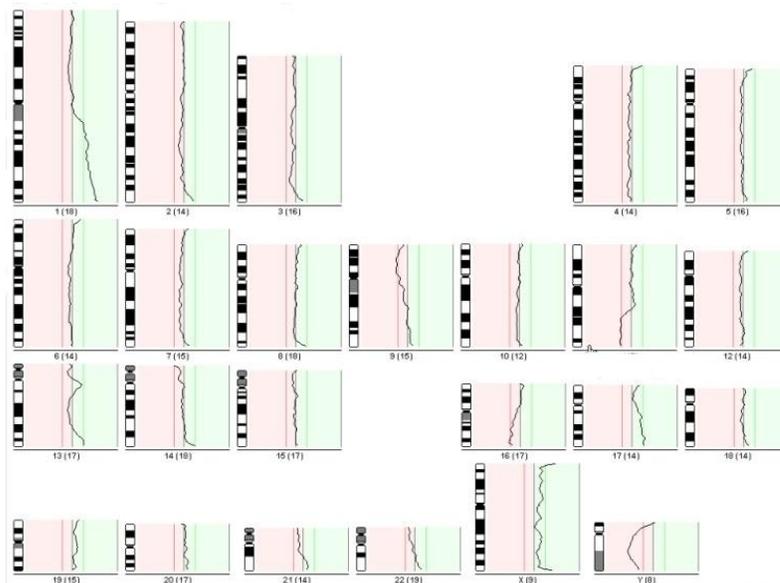
FIGURE 4. An example of a typical copy number profile derived as a result of cCGH. The moving line shows detected copy number changes. (http://www.lucia-cytogenetics.com/index.php?inc=cgh&lang=en)

Because of the low resolution of chromosomal CGH (cCGH) and the need for a direct measurement of specific genes genomic microarrays were developed. The first array based CGH method was published by Solinas-Toldo et al. in 1997 (Solinas-Toldo et al., 1997). They used genomic DNA clones derived from PAC vectors as the immobilized probe for differentially labeled test and reference DNA and achieved a resolution of 75-130Kb. Later on in 1998 Pinkel et al. investigated the performance of array CGH (aCGH) when such large PAC, BAC or Cosmid clones are used as probes and found that the method can effectively be

used to find copy number alterations related to cancer (Pinkel et al., 1998). The use of large on average 200Kb genomic clones however also had restrictions, such arrays covered the human genome only partially and the large scale purification of these clones from artificial chromosome vectors was laborious (for review see Mantripragada et al., 2004). Therefore in 1999 Pollack et al. developed a cDNA based microarray for copy number variation analysis (Pollack et al., 1999). They used cDNA clones and expressed sequence tags (EST) that were radiation hybrid mapped to chromosomal locations as the immobilized probe and were thus able to make a genome wide scan of copy number alterations. The advantages of using cDNA clones were greater resolution, good availability of cDNA clones and the possibility to make parallel expression analysis using the same array. However, also cDNA clones were restricted to some extent because they allowed copy number detection of only protein coding genes and no gene regulation regions were included in the array (for review see Mantripragada et al., 2004; for review see Pinkel and Albertson, 2005). Thus a further improvement followed in 2004 when oligonucleotide arrays were first described (Barrett et al., 2004; Carvalho et al., 2004). Oligonucleotides 50-60 base pairs in length can be designed for any genomic element and they can be printed on the array so that they provide an even or desired distribution of human genome. Oligos of known disease genes can be favored or the array can be designed so that it best represents normal human genome.

The CGH protocol is based on competitive binding of the test and reference DNA on to the immobilized probe. As the test and reference DNA are labeled with different fluorochromes the ratio of their intensities will stand for normal, underrepresented or overrepresented DNA. The fluorochromes usually used in aCGH are Cy3 (red) and Cy5 (blue) which at image analysis are given pseudo colors of green and red respectively. The difference between cCGH and aCGH protocol in terms of coloring is that in aCGH the sample is represented by red pseudo color and the reference with green pseudo color whereas in cCGH the labeling is vice versa. Once the DNA is labeled and the unincorporated label has been removed the sample and reference DNA are mixed. The mixture is then applied on the probe and as the hybridization takes place the sample DNA competes with reference DNA for the binding to each probe. As a result of this competitive hybridization probes that have more reference than sample DNA bound represent areas of copy number loss and probes that have

more sample than reference DNA bound represent areas of copy number gain. Probes that have the same amount of sample and reference DNA bound have no copy number change. For the accuracy of CGH it is crucial that there is an equal amount of sample and reference DNA in the hybridization mixture so that the competition over binding truly represents differences in the sample DNA relative to the reference DNA.

In order to determine how the DNA has bound to the probes the labels that were incorporated to DNA are excited to emit fluorescence and the intensity of fluorescence signal is measured. The two labels emit fluorescence on different channels Cy3 representing reference DNA on a green channel and Cy5 representing sample DNA on a red channel. A ratio of these two intensities is calculated by dividing the intensity of red channel with that of green channel (R/G) and this ratio then gives us a measure of bound DNA. The linear intensity ratios are often transformed to log2 ratios because linear ratios give unbalanced figures to lost and gained probes whereas logarithm base 2 provides a balanced measurement. On a linear scale a gene that has a copy number gain of factor 2 has an intensity ratio of 2 whereas a lost gene by the same factor has an intensity ratio of -0.5. When the ratios are transformed to log2 the figures change so that a copy number gain of factor 2 has a log2 ratio of 1 and a lost gene by the same factor has log2 ratio of -1. The probes with no copy number change represent normal DNA and have a log2 ratio of 0 (for review see Quackenbush, 2002). Transformation to log2 scale makes it easier to compare ratios and spot copy number imbalances. Figure 5 represents a schematic outline of both chromosomal and array CGH.

A. Schematic outline of CGH to metaphase chromosomes and genomic microarray
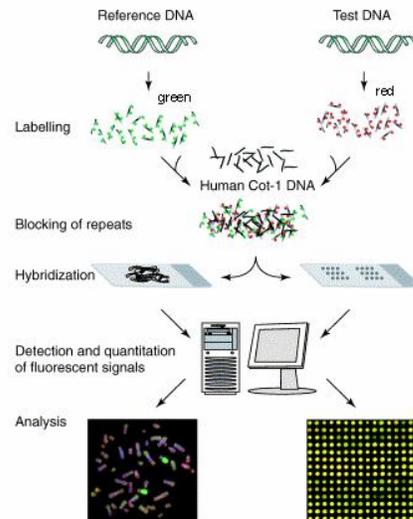
B. array CGH plot of log2 ratio and kb location
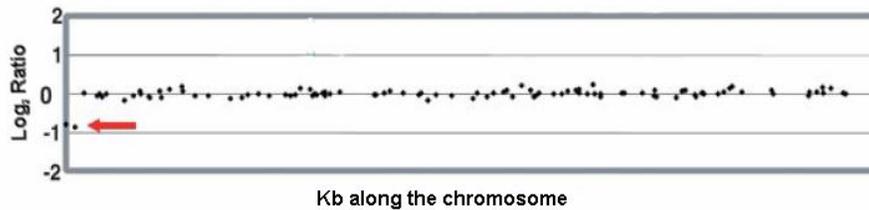
FIGURE 5. A) Schematic presentation of CGH protocol on metaphase chromosomes and genomic microarray B) An example of aCGH result; a plot of log2Ratio and kb location concerning one chromosome. The arrow points out the only detected copy number loss on this chromosome. (for review see Mantripragada et al., 2004; for review see Pinkel and Albertson, 2005)

As described earlier the change of probe from metaphase chromosomes through large genomic clones and smaller cDNA clones to oligonucleotides has step by step improved the resolution and accuracy of comparative genomic hybridization. The introduction of array based CGH however also brought some problems that needed to be resolved. The human genome contains repetitive DNA in the form of centromeric and telomeric repeats as well as tandem and interspersed repeats. The hybridization to these elements on such probes that contain these elements will result in data interpretation difficulties due to large amount of unique hybridization signals. Genomic and cDNA clones contain repetitive DNA and therefore the hybridization of repetitive DNA must be blocked, this is usually done by adding

unlabeled Cot-1 DNA to the hybridization mixture. Cot-1 is led to hybridize with repetitive elements thus blocking these sites from labeled sample and reference DNA. In addition technical difficulties on data analysis were introduced. The intensity and specificity of hybridization signals is crucial for accurate copy number detection. Signal intensities and array resolution are affected by the complexity of both genomic DNA applied on the probe and the probe DNA itself. More complex probes provide higher signals and therefore give more precise intensity measurements. Similarly the complexity of probe affects the specificity of hybridization. Genomic BAC clones have low complexity and oligonucleotides have high complexity so the resolution and specificity has increased by the advent of new array platforms. The difficulty of data analysis increases as the detection of single copy alteration has become possible as opposed to copy number alteration of larger genomic area. Also the magnitude of aberration is easier to detect if the imbalance is of higher magnitude. Moreover the genomic DNA applied on probe can vary from homogeneous cell line samples to heterogeneous tumor samples containing traces of normal cells. These factors affect the difficulty of data analysis and require more stringent interpretation of results as outline in Figure 6.
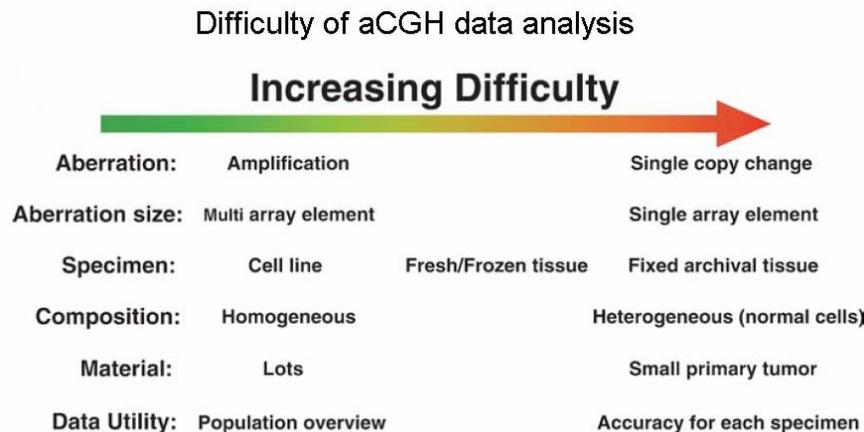

FIGURE 6. aCGH variables and the difficulty of data analysis. (for review see Pinkel and Albertson, 2005)

In addition to copy number identification in cancer and other diseases the method of aCGH can be used to detect normal copy number variation between individuals and to analyze

gene dosage abnormalities in developmental genetics. Copy number polymorphism and the identification of polymorphic sites facilitate the exclusion of such sites from copy number aberrations studies (for review see Pinkel and Albertson, 2005).

1.2 Gastrointestinal Stromal Tumor (GIST)

Cancers are divided into carcinomas, sarcomas, leukemias and lymphomas according to the tissue of origin. Carcinomas arise from the epithelium, sarcomas from mesenchyme, leukemias from hematocytic tissue and lymphomas from lymphatic tissue. Gastrointestinal stromal tumor (GIST) is a sarcoma. Moreover it is the most common tumor in the group of mesenchymal tumors of gastrointestinal tract. GIST is diagnosed in patients ranging from young adults to the elderly; the peak age of patients is approximately 60 years. The tumor can occur at any location within the gastrointestinal (GI) tract from the esophagus to the rectum. In addition to these locations GIST has also been reported at mesentry, omentum and retroperitoneum (for review see Corless et al., 2004; for review see Fletcher et al., 2002). The symptoms of GIST include abdominal pain, gastrointestinal bleeding and anemia however in many cases the tumor is found incidentally during laparoscopy (Gervasio et al., 2006; Sanchez et al., 2005; Ludolph et al., 2006).

Historically the diagnosis of GIST has been controversial because it was not distinguished from leiomyomas and leiomyosarcomas until 1980's by the advent of immunohistochemistry. Even after that it was not clear whether GISTs were a separate entity of tumors or a general group of tumors within the gastrointestinal tract including also leiomyomas and schwannomas (for review see Fletcher et al., 2002). This situation was finally clarified in 1998 when Hirota et al. firstly found that gastrointestinal stromal tumors harbored a gain of function mutation in the *KIT* proto-oncogene and secondly Sarlomo-Rikala et al. described an immunohistochemical marker CD117 for the product of this gene: KIT receptor. It thereafter became evident that GISTs arise from the intestinal cells of Cajal (IIC) which form a ring like wall of cells in the stomach and intestines and act as pacemaker cells responsible for peristalsis i.e. the movement of pulp from the stomach to the intestines. These cells require the expression of *KIT* proto-oncogene for their normal function and therefore

always label positively for CD117. GIST develops in the mesenchyme from IIC cells by a mutation that activates the KIT receptor and the cancer cells can thus be distinguished from normal mesenchymal cells by CD117 labeling. It is now widely accepted that GIST is a separate entity of tumors in the GI tract. It originates from *KIT* mutation that leads to a constitutive expression of KIT protein which is a tyrosine kinase receptor. As a result the KIT receptor, responsible for activating signaling pathways involved in cell proliferation, is turned on without the binding of its ligand stem cell factor (SCF). The expression of KIT and resulting positive labeling with CD117 marker has become the gold standard for the diagnosis of GIST. CD117 labeling also clearly separates GIST from leiomyomas and schwannomas which do not express KIT (for review see Fletcher et al., 2002; Hirota et al., 1998; Kindblom et al., 1998; Sarlomo-Rikala et al., 1998b).

Histologically GIST- tumors are of three phenotypes: spindle cell-, epithelioid cell and mixed cell type. These types are distinguishable by hematocyclin and eosin (H&E) staining after which the spindle cell type shows a characteristic uniform pattern of cells arranged in fascicles, the epithelioid type shows a pattern of rounded cells and the mixed type has characteristics of both types either in transition or commingling. These histological patterns are a helpful tool for pathologist in the preliminary diagnosis of GIST (see Figure 7) (for review see Fletcher et al., 2002).
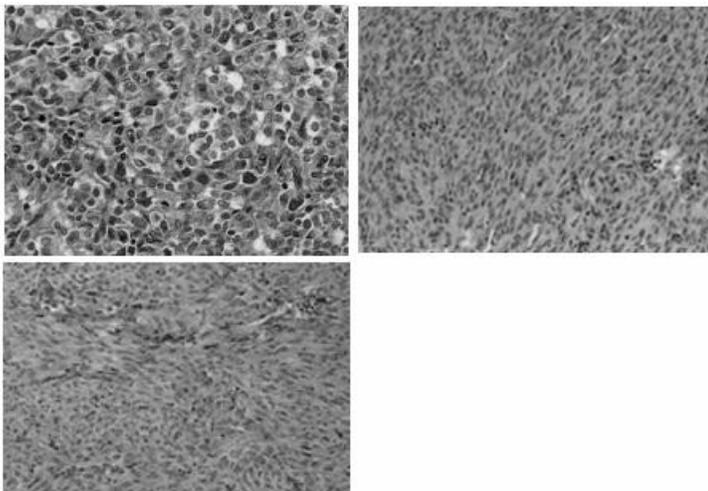

FIGURE 7. Epithelioid (upper left), spindle cell (upper right) and mixed cell (lower left) morphology of GIST. (for review see Fletcher et al., 2002)

After microscoping the confirmation of diagnosis is done by CD117 labeling. In summary the diagnosis of GIST is made using three indicators: clinical findings, morphological features at light microscopy and immunohistochemistry (Dematteo et al., 2002; for review see Fletcher et al., 2002; for review see Miettinen et al., 2002). In addition to CD117 also a few other immunophenotypic markers are frequently used in the diagnosis of GIST. Approximately 60% to 70% percent of GISTs label positively for CD34 a transmembrane glycoprotein normally expressed on endothelial cells and on hematopoietic stem cells. Some GISTs express smooth muscle actin (SMA) and S-100 protein detected by these markers. However, none of these additional antigens are specific for GIST. Sometimes it may be important to perform immunohistochemistry against desmin which typically is not expressed in GIST (for review see Fletcher et al., 2002). Immunohistochemistry is important in the diagnosis of GIST and labeling with various antibodies can help distinguish GISTs from other related tumors as can be seen from the table below.

TABLE 1. Immunohistochemical markers used in the diagnosis of GIST and related tumors. (for review see Fletcher et al., 2002)

Tumor	KIT (CD117)	CD34	SMA	Desmin	S-100
GIST	positive	positive (60% - 70%)	positive (30% - 40%)	very rare	positive (5%)
Smooth muscle tumor	negative	positive (10% - 15%)	positive	positive	rare
Schwannoma	negative	usually positive	negative	negative	positive
Fibromatosis	disputed*	rare	positive	rare cells	negative

Abbreviation: SMA, smooth muscle actin
* most often reported negative but not all authors agree

It should however be noted that despite its diagnostic importance not all GISTs label positively for CD117. Most studies report a positive CD117 labeling in between 85% to 90% of the cases analyzed (Goettsch et al., 2005; Sarlomo-Rikala et al., 1998b). According to Fletcher et al. there are only rare exceptional cases which should be diagnosed as GIST without CD117 immunopositivity regarding that they have other clinicopathologic features of GIST. These exceptions can arise through sampling error or sample preparation error which leads to negative CD117 labeling because of fixation artifact or very small biopsy size. In

some cases it is possible that the cells have seized to express KIT due to treatment (for review see Fletcher et al., 2002). There is however a small proportion of tumors, approximately 2% - 4% of all GISTs that are typical GIST tumors which in fact lack KIT overexpression (for review see Fletcher et al., 2002; Medeiros et al., 2004). These GISTs are an interesting subgroup of tumors that are thought to arise from an alternative mutation in platelet derived growth factor alpha (*PDGFRA*). When this subgroup of GISTs was studied more thoroughly in 2003 by two independent research groups it was found that actually most if not all of the KIT negative GISTs have a mutation in *PDGFRA* and furthermore the mutations in *KIT* and *PDGFRA* are mutually exclusive i.e. occur in a either or manner (Heinrich et al., 2003b; Hirota et al., 2003; Yi et al., 2005). This finding together with a recent article by Rossi et al. which provides evidence that KIT negative GISTs can be distinguished from other soft tissue tumors by PDGFR immunohistochemical detection able more accurate diagnosis and better treatment for GIST patients in the future (Rossi et al., 2005).

Prognosis of GIST is usually made according to two main criteria: size of tumor and the amount of mitosis per 50 high power field (HPF). The latter is a microscopic method used by the pathologists to determine how aggressively the tumor cells divide i.e. their mitotic rate. Generally it can be said that tumors that are ≤2 cm in size with a mitotic activity not exceeding 5 mitoses per 50 HPF have a good prognosis. The significance or tumor size is however dependent on tumor location. GIST occurs most commonly in the stomach small intestine and rectum in the order indicated and it has been shown that prognosis is better for those tumors found in the stomach even if they are larger in size. Tumors in the small intestine tend to be more aggressive. Nevertheless it is difficult for the pathologists to determine which GISTs metastize and which will will not. Sometimes originally benign GIST with no mitotic activity will metastize and therefore all GIST patients should be followed up for a long period of (for review see Fletcher et al., 2002; for review see Miettinen et al., 2002). The two main metastatic modes of GIST are dissemination to intra-abdominal sites and metastasis to the liver, metastasis in the lymph nodes are rarely found in GIST. Commonly sarcomas that have a mitotic count between 20 and 50/50 HPF are designated as highly malignant sarcomas but GISTs rarely have such high rates of mitoses. Adversely GIST tends to advance slowly recurring or metastising even after 10 to 15 years after primary surgery. The following table

illustrates some proposed guidelines to be used in the evaluation of GIST malignancy (Dematteo et al., 2002; for review see Miettinen et al., 2002).

TABLE 2. Prognostic guidelines for GISTmalignancy. (for review see Fletcher et al., 2002; for review see Miettinen et al., 2002)

Guidelines for defining risk of GIST malignancy			
	Size of tumor (cm)	Mitotic count per 50 HPF	Tumor location
Very low risk	<2	<5	ni
Low risk	2-5	<5	ni
Intermediate risk	<5	6-10	ni
	5-10	<5	ni
High risk	>5	>5	ni
	>10	Any mitotic count	ni
	Any size	>10	ni
Probably benign	≤2	≤5	intestinal
	≤5	≤5	gastric
Probably malignant	>5	>5	intestinal
	>10	>5	gastric
Uncertain or low malignant potential	2-5	≤5	intestinal
	5-10	≤5	gastric

Abbreviations: HPF, high power field, ni, not identified
Size of tumor is established as the single largest dimension

In terms of treatment surgery is the main treatment for primary GISTs and in fact remained as the only effective treatment for also recurrent and metastatic GISTs until the advent of a small inhibitory molecule STI-571 (imatinib mesylate) in the late 1990's. Before that GIST was a very difficult tumor to treat because it responses poorly to conventional chemo- and radiation therapy. Furthermore, radiation can only seldom be used because the recurring tumor is often so diffuse that the toxic effect to neighboring organs limits its use (Dematteo et al., 2002). The aim of surgical treatment of primary GISTs is to completely remove the tumor and avoid rupturing the tumor during resection. GIST tumors are often soft and fragile and unfortunately tumor rupture either before or during the surgery is a poor prognostic factor. Even if the surgery is successful many patients still develop recurrent disease (Dematteo et al., 2002). In case of recurrent or metastatic GIST treatment options before STI-571 were limited to surgery, chemotherapy (intravenous or intraperitoneal), radiation therapy and arterial embolization to block tumor blood supply. Moreover according to a study by Mudan et al. in 1999 the median survival after resection of recurrent GIST was

only 15 months. Luckily a turn of events in cancer research between 1998 and 2001 lead to a discovery STI-571 that has since revolutionasized the treatment of GIST (Dematteo et al., 2002; Mudan et al., 2000).

In the late 1990's research in the field of leukemia revealed that there was a specific chromosomal aberration in chronic myeloid leukemias (CML). This was a translocation of chromosomes 9 and 22 also called the Philadelphia chromosome. The result of Philadelphia chromosome is that part of a *BCR*-gene from chromosome 22 is fused with part of an *ABL* gene on chromosome 9 creating a fusion of two genes. This fusion gene expresses a fusion protein named BCR-ABL; a protein with tyrosine kinase activity. Later on Brian Druker at the Oregon Cancer Institute together with the scientists at Novartis pharmaceutical company managed to identify a molecule (STI-571) that could selectively inhibit the kinase activity of BCR-ABL fusion protein and actually kill CML cells in vitro (Dematteo et al., 2002; Druker et al., 1996). These promising results in the field of leukemia research proved valuable also for GIST researchers. In 1998 Hirota et al. sequenced the *c-KIT* cDNA from GIST samples and found that they harbored a mutation in the coding region between the transmembrane and tyrosine kinase domains i.e. the juxtamembrane domain. They also demonstrated that these mutant KIT receptors were constitutively turned on without their ligand the stem cell factor (SCF) and furthermore when murine lymphoid cell lines were transfected by the mutant *KIT* they suffered malignant transformation. Afterwards it was established that STI-571 is not specific only to ABL and BRC-ABL receptors but it also inhibits KIT and PDGFR receptors. Finally Tuveson et al. confirmed with human GIST cells that STI-571 inhibits the mutant KIT resulting in decreased cell proliferation an eventual apoptosis of these tumor cells (Buchdunger et al., 2000; Dematteo et al., 2002; Hirota et al., 1998; Tuveson et al., 2001). This remarkable event was followed by a treatment of one patient with metastatic GIST with this drug STI-571 later named imatinib mesylate and sold under trade name Gleevec in the United States and Glivec in the rest of the world by Novartis, Basel, Switzerland. The first patient study was accomplished in Finland by professor Joensuu with very promising results. The 50-year old female patient had an aggressive metastatic GIST that was non-responding to chemotherapy. After one month of treatment with STI-571 the patient's tumor volume decreased 52% and the patient was alive and well after 11 months of treatment. Thereafter a comprehensive patient

trial on advanced GIST was prepared. The results showed that more than half of the patients responded to imatinib mesylate despite the fact that almost 14% of patient developed an early resistance to imatinib. Imatinib mesylate has since been approved by the US Food and Drug Administration (FDA) as an effective therapeutic agent for patients with unresectable or metastatic KIT-positive GIST (Demetri et al., 2002; for review see Hirota and Isozaki, 2006; Joensuu et al., 2001).

The development of imatinib and the research underlying it started a new era in cancer research. Before imatinib the drugs designed for cancer patients had all been non-specific drugs that also affected the normal cells of the body. These chemotherapy agents were designed to kill proliferating cells with drastic side effects. Also drugs that alleviated the effects of chemotherapy were developed. After the discovery of a specific, molecularly targeted drug imatinib mesylate cancer research has focused on understanding the molecular behavior of cancer cells in order to develop targeted drugs against them (Dematteo et al., 2002). Moreover treatment of GIST was drastically enhanced by the discovery of imatinib. Earlier the fate of GIST patient with recurrent disease was often fatality because there was no effective therapy for metastatic disease. Despite the good progress it is now known that not all GIST patients respond to imatinib and some that do initially respond develop resistance to the drug later on. The research in the field is now concentrating on finding out reliable markers that can be used when making a decision whether or not patient is eligible to imatinib treatment. Also the molecular mechanisms underlying drug resistance together with clinical trials on drug dosage are investigated (Dematteo et al., 2002; Joensuu et al., 2001; Medeiros et al., 2004; Zalcberg et al., 2005).

The problem that still remains in the treatment and diagnosis of GIST concerns the subgroup of tumors that are immunohistochemically negative for KIT. This group comprises about 10% – 15% of GIST and about half of them have been shown to contain alternative mutation in *PDGFRA* gene as described earlier in these thesis. These patients need to be correctly diagnosed as GIST patients with the help of PDGFRA immunohistochemistry and/or mutational analysis of *KIT* and *PDGFRA* genes and yet imatinib is currently approved for use to KIT positive GIST patients only. Patients with *PDGFRA* mutation need to be entered into clinical trials. In addition approximately 5% of KIT negative GIST patients do not have a

mutation in either *KIT* or *PDGFRA* genes. The mechanism underlying the pathogenesis of these GIST remains to be investigated (Debiec-Rychter et al., 2004; for review see Hirota and Isozaki, 2006; Rossi et al., 2005).

1.2.1 *KIT* and *PDGFRA* mutations and the molecular mechanism of Glivec

The *c-KIT* proto-oncogene is a cellular homolog for *v-KIT* originally identified from a Hardy-Zuckerman 4 feline sarcoma virus (HZ4-FeSV) in 1986 by Besmer et al. The gene product of *KIT* is a transmembrane tyrosine kinase receptor closely related to other tyrosine kinases such as the platelet derived growth factor (PDGFR) and colony-stimulating factor-1 (CSF-1) which also have oncogenic capabilities. Stem cell factor (SCF) is the ligand of KIT, the binding of it into the receptors enzymatic site induces a homodimerization of two adjacent KIT receptors. Homodimerization is followed by autophosphorylation event in which the adjacent receptors phosphorylate each others intracellular domain. This in turn activates other cellular proteins to join the receptor and these proteins activate cellular pathways involved in mitosis, chemotaxis, adhesion, apoptosis and cell differentiation. The following figure demonstrates these pathways in more detail (Besmer et al., 1986; Blume-Jensen et al., 1991; for review see Heinrich et al., 2002; Majumder et al., 1988).
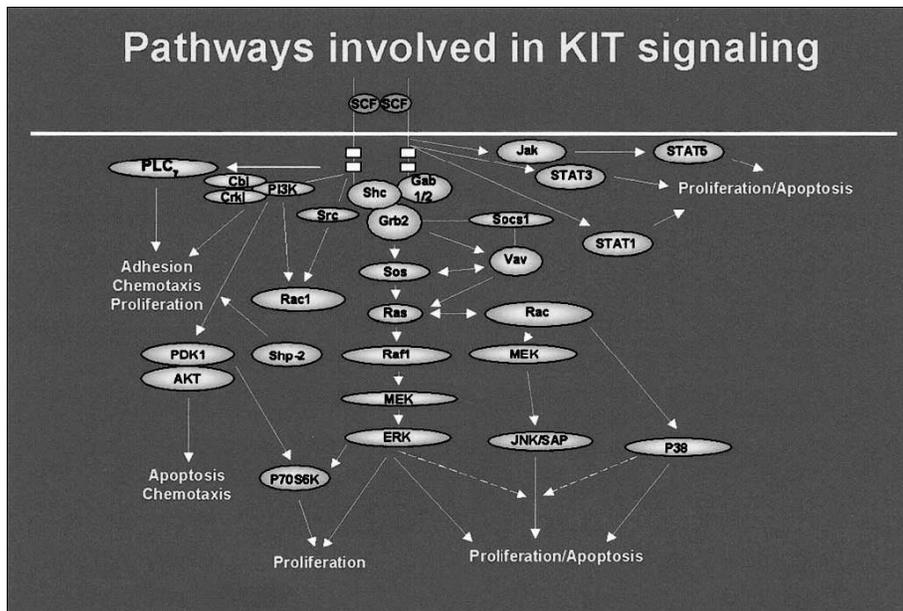
FIGURE 8. KIT signaling pathways. (for review see Heinrich et al., 2002)

The coding sequence of *KIT* gene consists of 21 exons. Mutations related to GIST are reported in four of these exons namely exons 11, 9, 13 and 17. Exon 11 codes for the juxtamembrane domain of KIT located right after the cytoplasmic site of the receptor. The juxtamembrane domain is crucial for signal transduction because this domain interacts with adapter proteins and is involved in the catalytic activity of KIT by administering the active and inactive conformation of the receptor. Exon 9 codes the extracellular region of KIT and exons 13 and 17 code for tyrosine kinase domains located in the intracellular part of the receptor (Antonescu et al., 2005; Hirota et al., 1998; Rubin et al., 2001). The mutations demonstrated include base pair substitutions, deletions and duplications which however almost always preserve the open reading frame of the genes involved. Exon 11 mutations are most common occurring in 70% to 85% of GISTs followed by exon 9 which is mutated in up to 13% of GISTs. Together the non exon 11 mutations comprise a substantial subgroup of mutations. Overall *KIT* is mutated in up to 92% of all GISTs and evidently KIT is activated also in those GISTs that do not demonstrate a *KIT* mutation (for review see Hirota and Isozaki, 2006; Rubin et al., 2001). Exon 11 mutations were verified to cause a ligand independent activation of KIT early on in 1998 and later on it has been established that in fact mutations in all KIT domains are coupled with high level KIT activation by phosphorylation. According to Rubin et al. there

is no significant correlation between different *KIT* mutations and the malignancy of the tumor and they therefore suggest that oncogenic gain of function mutations are an early event in the pathogenesis of GIST. This hypothesis is supported by Hirota and Isozaki who argue that these mutations and the resulting ligand independent activation of KIT receptor is the cause of GIST (Hirota et al., 1998; for review see Hirota and Isozaki, 2006; Nakahara et al., 1998; Rubin et al., 2001). The structure of KIT receptor together with the activating mutations and their frequency is outlined in Figure 9.
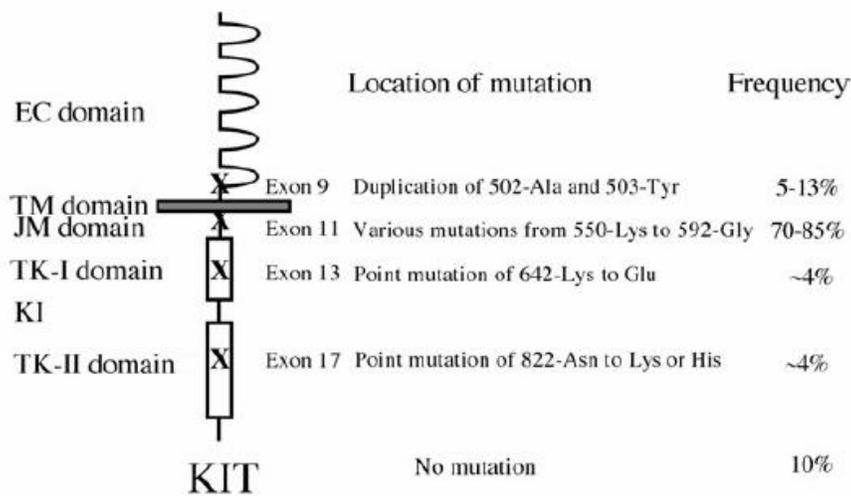
FIGURE 9. Structure of KIT receptor. Abbreviations: EC, extracellular; TM, transmembrane; JM, juxtamembrane; TK, tyrosine kinase; KI, kinase insert. (for review see Hirota and Isozaki, 2006)

An alternative mutational mechanism causing GIST involves the PDGFRA receptor which is structurally similar to KIT (see Figure 10). The mutations in the *PDGFRA* gene are detected in exons 12 and 18 located at the juxtamembrane and tyrosine kinase domains respectively. These mutations are gain of function by nature and the exons correspond to exons 11 and 17 in the *KIT* gene. The most frequent mutation in *PDGFRA* gene is observed in exon 18 (Heinrich et al., 2003b; Hirota et al., 2003).
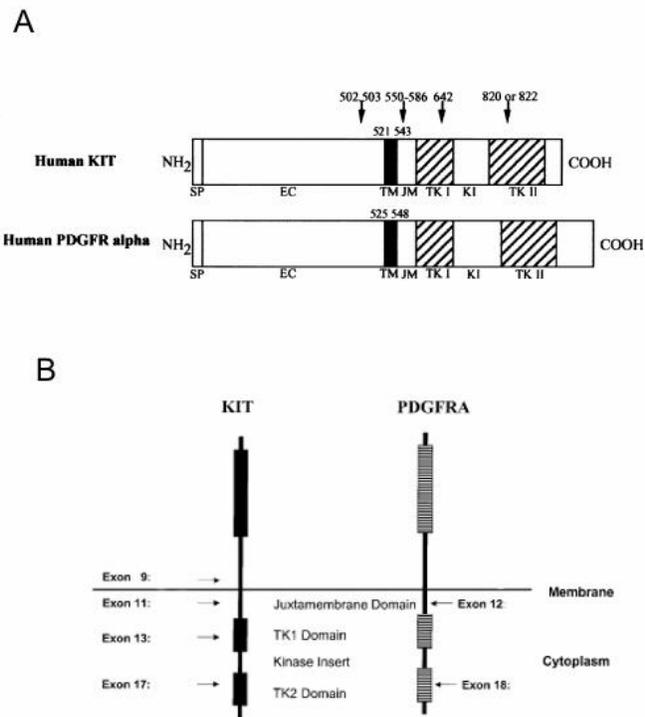
FIGURE 10. Comparison of KIT and PDGFRA receptor proteins. A) protein level B) cellular level. Abbreviations: EC, extracellular; TM, transmembrane; JM, juxtamembrane; TK, tyrosine kinase; KI, kinase insert. (Heinrich et al., 2003a; Hirota et al., 2003)

Imatinib mesylate is a small synthetic molecule which inhibits both KIT and PDGFRA receptors. Imatinib is a competitive inhibitor of these receptors i.e. it binds to the same enzymatic site as the normal ligands of these receptors. The binding of imatinib however renders the receptor inactive by inhibiting the autophosphorylation event normally followed by the binding of correct ligand (Debiec-Rychter et al., 2004; Heinrich et al., 2003a). The inhibitory mechanism of imatinib was characterized in molecular level by Mol et al. in 2004 when they reported the crystal structures of both native *KIT* and *KIT* with bound imatinib (see Figure 11). These structures also provided further insight into the mechanism of KIT activation. It was revealed that the mutations described earlier result in constitutive activation of KIT because they interfere with the autoinhibitory function of the receptor. The juxtamembrane domain of the receptor interacts with the kinase domain by either maintaining an inactive or active conformation. Thus the juxtamembrane region has two roles; it has an

autoinhibitory function when unphosphorylated and an activating intracellular signaling function when phosphorylated (Antonescu et al., 2005; Mol et al., 2004). Mutations in few crucial amino acids either in the juxtamembrane domain or in activation loop destabilize the autoinhibited, inactive conformation of the receptor and this is the cause of constitutive activation. Additionally it was shown that imatinib actually binds to the inactive KIT receptor and stabilizes an inactive conformation that is somewhat different from the autoinhibitory conformation. This finding led to a conclusion that there can be at least two mechanisms which lead to resistance of imatinib treatment. First, secondary point mutations may lead to the stabilization of active conformation which does not bind imatinib and secondly, additional mutations may alter the protein structure so that it disrupts imatinib binding without affecting the conformation of KIT (Antonescu et al., 2005; Mol et al., 2004).
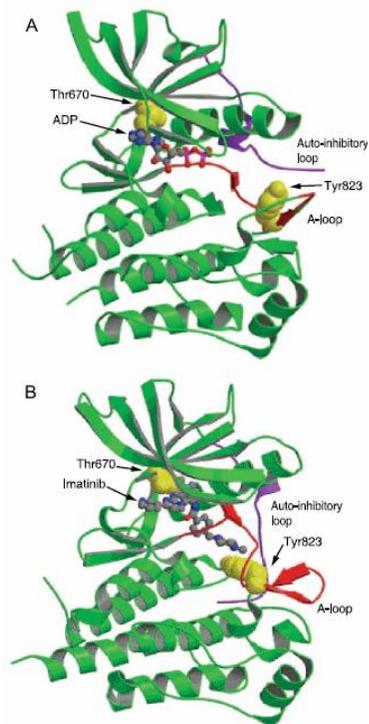
FIGURE 11. Protein structure of KIT interacting with imatinib. A) Active conformation with ADP bound. B) Inactive conformation with imatinib bound. (Antonescu et al., 2005)

Some patients are resistant to imatinib from the start of treatment and some acquire resistant later on. Primary resistance occurs when patient does not respond to imatinib treatment originally and secondary resistance occurs when patient after varying degree of initial response suffers a relapse after weeks or months of treatment. In 2003 Heinrich et al. showed correlation between different *KIT* mutations and initial response to treatment with imatinib. They found that patients with exon 11 mutations were more likely to respond to imatinib than patients with exon 9 mutations or patients without *KIT* or *PDGFRA* mutations. In terms of *PDGFRA* mutations they found that a specific substitution at codon 842 which changes aspartic acid to valine (D842V) seems to be primary resistant to imatinib whereas other known mutant isoforms of *PDGFRA* are sensitive to imatinib. As postulated in the previous paragraph and investigated by at least two patient studies, the cause of secondary resistant evidently turned out to be a second mutation acquired after the beginning of imatinib treatment. This second mutation occurs frequently in exon 17 of *KIT* but can also appear in *PDGFRA* gene (Debiec-Rychter et al., 2005; Wakai et al., 2004). To conclude it can be said that mutations underlying the pathogenesis of GIST can be divided into two types: enzymatic site (ES) and regulatory type (RT) mutations. Mutations that affect the enzymatic domain of either *KIT* or *PDGFRA* actually interfere with imatinib binding and are thus related to poorer prognosis than those affecting regulatory domains of these receptors. It has been confirmed that imatinib is effective against regulatory type mutants of KIT but the ES mutants seem to be primary resistant to it. These findings further support the need for mutational analysis of GISTs when making treatment decisions. It is however good to bear in mind that most GIST patients have regulatory type exon 11 mutations and they respond well to imatinib treatment (Debiec-Rychter et al., 2005; Ma et al., 2002).

1.2.2 Cytogenetic findings in GIST

In addition to mutations other changes in the genetic material of GIST patients can be studied. Research on chromosomal aberrations either in copy number or structural changes can be a useful tool in identifying genetic markers and possible oncogenes. Translocations are associated with many cancers and some cancers e.g. CML are characterized with a specific

translocation. Translocations contribute to tumorigenesis via altered gene regulation or creation of oncogenic fusion genes. They are perhaps the most important genetic alterations contributing to the etiology of cancer although in recent years other genetic alterations such as losses and gains of genetic material have also provided new insight to cancer pathogenesis (for review see Bennicelli and Barr, 1999). Cancer is a genetic disease and in addition to sporadic cancers i.e. cancers arising from somatic changes there are also familial cancers that arise from mutations in the germline. Some hereditary cancer syndromes have been a useful research tool since it has been shown that the same genes tend to be mutated in both sporadic and familial cancers. Thus genes that can be more easily identified in rare hereditary cancer syndromes are good research targets of sporadic cancers as well. GIST also exists as a familial syndrome and indeed it has been established that germline *c-KIT* mutation is the cause of familial GIST (Fearon, 1997; Nishida et al., 1998). Interestingly despite of germline *KIT* mutation these patients do not develop GIST until at adulthood. This clinical observation clearly suggests that there must be additional genes involved in the pathogenesis of GIST. Cytogenetic findings in relation to GIST can help understand the molecular progression of GIST and provide important indications to the location of these genes (Isozaki et al., 2000).

In 1996 El-Rifai et al. performed a comparative genomic hybridization of GIST on metaphase chromosomes and found a recurrent loss of DNA copy number in chromosome 14, in the q-arm. This loss was found in 75% of benign and in 62% of malignant samples indicating that this loss in an early event in the development of GIST. The minimal common overlapping area of copy number loss in their series was defined at 14q22 and importantly possible existence of a tumor suppressor gene at this location was suggested. They also established that copy number losses in GIST seemed to be more frequent than gains and that amplifications were more common in malignant than in benign GISTs. High level amplifications were found at 3q26-q29, 5p and 8q22-q24 (El-Rifai et al., 1996). These observations were later confirmed by several studies. In 1998 Sarlomo-Rikala et al. used cCGH to compare the copy number profiles of GIST and related tumors. They found copy number losses at 14q in 77% of GIST samples and other frequent losses at chromosomes 22, 15 and 1p. Furthermore, the copy number loss at 14q was not found in related smooth muscle tumors such as leiomyomas and schwannomas and it was determined to be another reliable

marker differentiating GIST from these tumors. Later during the same year Knuutila et al. performed cCGH using pooled DNA of different GIST samples. They confirmed losses at 14q and 1p and refined the loss of 22q to a region at 22q12. Furthermore, they found a loss at 13q21-q31 and gains at 5p, 8q22-q24, 17q22-qter and 19q13. In 1999 O'Leary et al. conducted a LOH study on chromosome 1p and found that allelic loss of 1p36 correlated with shorter survival of GIST patients. They suggested that a tumor suppressor with prognostic value may be located at this region (for review see Corless et al., 2004; Knuutila et al., 1998; O'Leary et al., 1999; Sarlomo-Rikala et al., 1998a). Soon after additional copy number changes and loss of heterozygosity regions were identified. Most frequent findings were the loss of 1p, 14q and 22q with occurrence of approximately 25%-51%, 74%-75% and 50%-53% respectively. Gains were reported to occur less frequently and were also associated with malignancy; reported areas include 8q, 17q, 20q and 5p. LOH was associated with chromosomal regions of 14q and 22q (El-Rifai et al., 2000a; Fukasawa et al., 2000; Knuutila et al., 1998). Few studies attempted to relate chromosomal aberrations to the prognosis of GIST with somewhat controversial results. El-Rifai et al. correlated losses of 9p, 13q, 15q and 19q as well as gains of 5p, 8q, 17q and 20q with malignant behavior. They suggested the involvement of *c-MYC* at 8q and *ERBB2* at 17q in prognosis of GIST. In addition Kim et al. proposed loss of 22q to be a marker for poor prognosis and anomalism of 1p was associated with malignancy by Breiner et al. Controversially El-Rifai et al. did not relate losses of 1p and 22q with prognosis and furthermore Breiner et al. claimed that both 14q and 22q losses were an early event in GIST development. It was however clear that the presence of gains as well as an accumulating number of aberrations was related to malignant transformation in GIST (Breiner et al., 2000; El-Rifai et al., 2000a; Kim et al., 2000).

It became evident that loss of 14q, seen in equal proportions in both benign and malignant GISTs in several studies, must be an early event in the pathogenesis of GIST, however bearing in mind the importance of *KIT* mutation. Loss of 22q was another recurrent aberration reported. Many studies made assumptions on tumor suppressor genes harbored at the copy number loss regions and at the same time minimal overlapping areas of these sites were reported. Copy number loss at 14q was further distinguished by El-Rifai et al. in 2000 when they identified two distinct sites of copy number losses in this chromosome. They

performed both cCGH and LOH analysis on 30 GISTs and by combining the results of both methods located recurrent deletions at 14q11-q12 and 14q23-q24.3. They concluded that since these regions are interrupted by normal sequences there must be two tumor suppressor genes acting together in the development of GIST. These findings were confirmed and further defined by Debiec-Rychter et al. by FISH analysis. They found three separate deletion regions on chromosome 14: 14q11-q12, 14q22-q23 and 14q24.3 (Debiec-Rychter et al., 2001b; El-Rifai et al., 2000b; Gunawan et al., 2002; Kim et al., 2000). None of these methods however allowed detection of the possible tumor suppressor genes and no such genes were known to be located at 14q. However, El-Rifai et al. speculated that a DNA repair enzyme coded by *APEX* gene might be involved since it is located at one of the regions they identified at 14q and Debiec-Rychter et al. considered the role of *FOS* oncogene at 14q24.3. Furthermore, Fukasawa et al. stated that *NF2*, a known tumor suppressor, could act in those GISTs that have either a copy number or allelic loss of 22q. A loss of 9p was investigated by Kim et al. and they made an assumption that p16^{INK4A} gene could be the target of this aberration (Debiec-Rychter et al., 2001b; El-Rifai et al., 2000b; Fukasawa et al., 2000; Kim et al., 2000).

Chromosome 22 was investigated specially in relation to *NF2* in which Fukasawa et al. had actually found a mutation in GIST. The product of *NF2* is merlin which is inactivated in some cancers e.g. schwannomas. Pylkkänen et al. studied allelic loss of 22q in conjunction with merlin expression and found that even though LOH at *NF2* locus was very frequent these tumors were immunopositive for merlin. Furthermore, *NF2* was not mutated in any of their samples and they thus concluded that *NF2* may not be important in GIST pathogenesis. These results were recently confirmed by Lasota et al (Fukasawa et al., 2000; Lasota et al.; 2005; Pylkkanen et al., 2003). Moreover it was declared that there is no correlation with genetic instabilities and *c-KIT* mutation. Genetic changes rather represent a complimentary molecular mechanism of GIST pathogenesis and the locations where aberrations are frequently found implicate independent action of yet unidentified tumor suppressors and/or gene repair genes. Nevertheless Debiec-Rychter et al. did find a correlation between loss of 9p and *c-KIT* mutation as well as 1p loss and wild type *KIT*. They suggested that these findings may represent different pathways used in the progression of GIST (Debiec-Rychter et al., 2001a; Fukasawa et al., 2000). In 2001 a GIST workshop was held at the National Institute of Health

(NIH), it lead to a special article series published in Human Pathology vol 33, No. 5 in May 2002. In one of these articles Heinrich et al. stated for the first time that genetic alterations indeed are most likely preceded with *c-KIT* mutation followed by accumulating cytogenetic changes as the disease progresses. Furthermore, he suggested a general outline for the genetic progression of GIST: KIT mutation → loss of 14q → loss of 22q → loss of 1p → gain of 8q → loss of 11p → loss of 9p → gain of 17q. He also implicated that there might be alternative, non-mutational mechanisms for the activation of KIT such as amplification of *c-KIT*. Since then *KIT* amplification has been detected in few samples series however it seems that instead of amplification regulation of gene expression is a more likely alternative mechanism of KIT activation (Debiec-Rychter et al., 2005; for review see Heinrich et al., 2002; Tabone et al., 2005). Additionally Heinrich et al. made an important notion that in comparison to many other cancers GIST has a rather noncomplex cytogenetic profile with most frequent imbalances being the loss of 14q, 22q and 1p. In benign tumors loss of 14q is sometimes observed as the only aberration. This non-complexity enables efficient research aimed at the few important chromosomal regions and the genes targeted by them. At the same time it allows the use of cytogenetics as a complimentary tool in diagnostics and prognosis. Figure 12 compares the karyotypes of GIST and leiomyosarcoma.
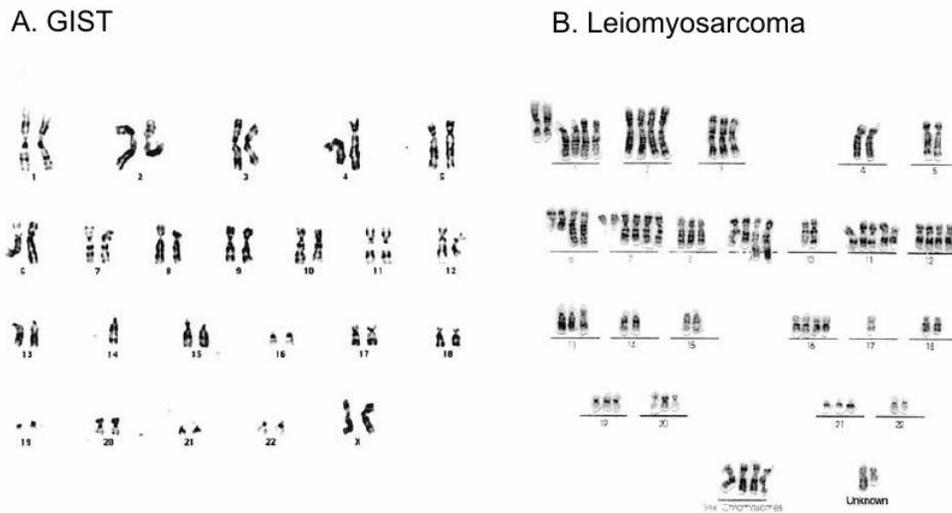
FIGURE 12. Karyotype of A) GIST and B) Leiomyosarcoma. The karyotype of GIST shows a monosomy of chromosome 14 as the only aberration whereas leiomyosarcoma has many gains losses and chromosomal rearrangements. (Heinrich et al., 2002)

Cytogenetic studies on GIST have revealed that the cytogenetic profile of GIST is different from related smooth muscle tumors supporting the recognition of GIST as a distinct entity of tumors. Other consistent findings have indicated that losses of genetic material are more common than gains, accumulating number of aberrations and the presence of gains is related to the progression of GIST and loss of 14q, being the most frequent finding in both benign and malignant tumors, is involved in the development of GIST. Regardless of FISH, LOH and cCGH studies the genes targeted by chromosomal aberrations, underlying the molecular progression of these tumors remain to be identified. Recently a tissue microarray study aiming to identify some of these genes was conducted. It explored the amplification of nine known oncogenes and found four of these amplified in the sample series. However, the occurrence of amplification was less than 10% in all of them and thus further research concerning the involvement of these genes is needed (Tornillo et al., 2005). To the best of my knowledge no array CGH study on sporadic GIST has yet been published, consequently the study made in conjunction with these thesis provides new information on target genes of genetic alterations in GIST.

2. Aim of the Study

The aim of this study was to apply the new and effective method of array CGH to the research of gastrointestinal stromal tumors and to understand the purpose of chromosomal imbalances through identification of their target genes. It was anticipated that the experiment would provide new information to explain the molecular pathogenesis of these tumors. Special emphasis was laid on chromosome 14 with an aim to define a smaller overlapping area of imbalance located in the q-arm. The goal was also to get direct copy number data of the genes indicated by previous reports as possible targets of chromosomal aberrations and to provide an overview of chromosomal imbalances in GISTs.

3. Materials and methods

The study consisted of laboratory work, data analysis and result interpretation. Figure 13 displays the workflow of the study.

Workflow of Comperative Genomic Hybridization
A. Laboratory work

Workflow of Comperative Genomic Hybridization
B.Data analysis

| DNA extraction and concentration measurement |
| Digestion and purification of DNA |
| Gel electrophoresis and concentration measurement |
| DNA labeling and hybridization to array |

| Feature Extraction Software 8.1 Extraction of feature intensities |
| GeneSpring 7/CGH Analytics 3.2 Data filtering and probe mapping to chromosomal locations |
| aCGH Smooth /CGH Analytics 3.2 Aberration breakpoint identification |
| Result interpretation |

FIGURE 13. Workflow of array CGH performed in current study.

3.1 Tumor Samples

Department of Pathology, University of Valencia, Spain provided 26 tumor samples to this study. The samples were shipped as formalin fixed paraffin embedded tissue sections. In addition Department of Pathology, Helsinki University Central Hospital provided 33 tumor samples provided as DNA extracted from either fresh frozen or formalin fixed paraffin embedded tumors. For reasons to be described later on in these thesis some samples were left out of the study and as a result the sample series of current study consisted of 35 tumor samples from patients diagnosed with GIST. In the series 20 samples represented malignant GISTs (57%) and 15 samples (43%) were benign GISTs, the age of patients ranged from 32 to 88 with a median of 60 years. Proportion of tumor cells in each sample was always between 60% and 80%. The percentage of tumor cells is important because cells from the surrounding healthy tissue may skew the results. The tumor cell content of sample should be at least 50%

for accurate comparative genomic hybridization. The clinical data of tumors is summarized in Table 3.

TABLE 3. Clinical data of tumor samples.

Sample	Loc	diameter cm	PAD	PAD	sex/age	mutation
1	stomach	4.5	GIST	benign	m/45	c-kit wt, PDGFRA exon 12
2	stomach	7	GIST	benign	f/61	c-kit wt, PDGFRA exon 12
3	stomach	3.3	GIST	benign	m/50	c-kit wt, PDGFRA exon 18
4	stomach	3	GIST	benign	f/65	c-kit exon 11, PDGFRA ne
5	stomach	5	GIST	benign	m/85	c-kit exon 11, PDGFRA ne
6	jejunum	2	GIST	benign	m/69	c-kit wt, PDGFRA wt
7	stomach	9	GIST	benign	f/67	c-kit exon 11, PDGFRA ne
8	stomach	6	GIST	benign	m/53	c-kit exon 11, PDGFRA ne
9	jejunum	7	GIST	benign	m/41	c-kit exon 11, PDGFRA ne
10	stomach	2	GIST	benign	f/60	na
11	stomach	4.5	GIST	benign	f/70	na
12	stomach	3.5	GIST	benign	f/60	na
13	jejunum	3.8	GIST	benign	m/67	na
14	gastric	<2	GIST	benign	f/72	c-kit exon 11, PDGFRA wt
15	gastric wall	na	GIST	benign	m	c-kit exon 11, PDGFRA wt
16	stomach	15	GIST	malignant	m/52	c-kit wt, PDGFRA wt
17	jejunum	10	GIST	malignant	m/60	c-kit exon 11, PDGFRA ne
18	stomach	6	GIST	malignant	f/88	c-kit exon 11, PDGFRA ne
19	stomach	17	GIST	malignant	m/44	c-kit exon 11, PDGFRA ne
20	jejunum	9	GIST	malignant	f/71	na
21	jejunum	9	GIST	malignant	f/73	na
22	stomach	10	GIST	malignant	f/46	na
23	colon mesentery	na	GIST	malignant	f/46	c-kit exon 11, PDGFRA ne
24	colon mesentery	na	GIST	malignant	f/46	na
25	abdomen metast	12	GIST	malignant	f/64	c-kit exon 11, PDGFRA ne
26	stomach	17	GIST	malignant	m/44	c-kit wt, PDGFRA wt
27	jejunum	15	GIST	malignant	m/54	c-kit wt, PDGFRA wt
28	stomach	8	GIST	malignant	f/74	na
29	jejunum	10	GIST	malignant	m/72	na
30	jejunum	12.5	GIST	malignant	f/39	na
31	omentum	3	GIST	malignant	m/32	na
32	abdomen metast	3	GIST	malignant	m/71	na
33	abdomen metast	2.5	GIST	malignant	f/42	na
34	small intestine	>2	GIST	malignant	m/54	c-kit exon 11, PDGFRA wt
35	retrovaginal	>5	GIST	malignant	f/52	c-kit exon 11, PDGFRA wt
wt= wild type na= not available						

3.2 DNA Extraction, Digestion and Purification

DNA was extracted from 26 samples provided by the University of Valencia. The formalin fixed paraffin embedded tissue sections were first deparaffinazed in a 15 ml Falcon tube by treating them with xylene (Merck; Darmstadt, Germany) for two times, 5 minutes each. After 5 minute centrifugation (Heraeus Multifuge 3s) at 1700 rpm the xylene traces were removed by absolute ethanol (Fysioline Pharma Oy; Tampere, Finland) treatment at 55°C two times 5 minutes followed by another centrifugation. The supernatant was discarded and the rest of ethanol evaporated at 55°C for approximately 1h. The cells were then lysed with lysis buffer (see appendix 1) and Proteinase K (Merck; Darmstadt, Germany) at 55°C for 17- 48h with interval mixing. Next an RNAase (Roche; Boehringer, Mannheim) treatment of 1h at 55°C was performed after which proteins were salted out (5M NaCl) and the DNA extracted from the supernatant by standard ethanol precipitation. Finally DNA was dissolved to 100µl of TE-buffer pH 8 (see appendix 1) Reference DNA was extracted from peripheral blood of healthy individuals. A separate male and female pool of peripheral blood was supplied by The Finnish Red Cross Blood Service. The extraction protocol has been described earlier (Miller et al., 1988) briefly 5 ml of blood was incubated with TKM1+Nonidet solution (see appendix 1) at room temperature for 10 minutes. The tubes were then centrifuged at 2500 rpm for 15 minutes (Heraeus Multifuge 3s) after which the supernatant was discarded and TKM1-buffer (appendix 1) was added. In order to fragment the pellet the tubes were shaken vigorously before centrifugation at 2500 rpm for 10 minutes. This step was repeated once. Next TKM2-buffer (appendix 1) and 20% SDS was added to break the nucleus membrane at 55°C over night. Proteins were then salted out with 5M NaCl after which DNA was precipitated with ethanol. Finally the visible DNA string was fished from the supernatant with a Pasteur pipette, washed with 70% ethanol to remove salt and dissolved to 150µl TE-buffer pH 8.

The quality of genomic DNA was carefully examined by Agarose Gel Electrophoresis and from the formalin fixed paraffin embedded tissue sections only eight samples were approved for the aCGH experiment. DNA tends to fragment during formalin fixation and therefore paraffin embedded archival tissue sections are not the best material for comparative genomic hybridization which requires intact DNA. The integrity of DNA is important because

to detect copy number imbalances the sample should represent complete genomic DNA of an individual. Degraded DNA is a poor representative of whole genomic DNA and the smallest fragments generated by degradation are able to hybridize with many targets skewing the results. Different genomic amplification methods have been described (Ghazani et al., 2006; Wang et al., 2004) but due to the possibility of errors in the amplification process it has been a standard protocol at the laboratory of cytomolecular genetics to use only non-amplified genomic DNA for aCGH. To prepare the DNA for aCGH digestion and purification of both reference and sample DNA was performed. Digestion was done to facilitate the labeling of DNA and purification to clear the DNA solution from the enzymes used for digestion as well as from other residual contaminants. For cDNA array 20 µg of genomic DNA was digested over night at 37°C with Alu I and Rsa I (Sigma-Aldrich; St. Louis, MO) to obtain DNA of uniform 500 bp lengths. The DNA was then purified by Phenol-Chloroform-method using Phase Lock gel tubes (Eppendorf AG; Hamburg, Germany) so that 1x volume of phenol: chloroform: IAA solution (25:24:1) was added to the tubes containing the digested DNA. The solution was mixed thoroughly and removed to Phase Lock gel tubes. The tubes were centrifuged at 10 000 rpm for 5 minutes (Eppendorf Centrifuge 5415R) after which the upper phase containing the DNA was pipeted into to a new tube in which the phenol treatment was repeated. Next 1/10 volume of 3M Na-acetate and 2x volume of absolute ethanol was added and the DNA was let to precipitate at -20°C for over night. The tubes were then centrifuged at full speed (16.1 rcf) for 30 minutes in order to pellet the DNA. To remove salt from the DNA the pellet was washed with 70% EtOH and let to dry. The purified DNA was dissolved into 35µl of TE-buffer pH 8. For oligoarray 10 µg of genomic DNA was digested as before but only for two hours. The purification was done using QIAprep Spin Miniprep kit (Qiagen GmbH; Hilden, Germany). After digestion and purification the size of DNA was checked by Agarose Gel Electrophoresis and the amount of DNA was measured by absorbance at 260 nm using a spectrophotometer (GeneQuant pro). The purity of DNA was evaluated by measuring the 260/280 absorbance ratios.

3.3 Labeling and Hybridization cDNA array

Labeling and hybridization was performed according to protocol described earlier (Atiye et al., 2005; Pollack et al., 1999). For each array 6 µg of both reference and tumor DNA was differentially labeled with Cy3-dUTP and Cy5-dUTP respectively (Amersham Biosciences; Piscataway, NJ) by random priming method using the RadPrime DNA labeling kit (Invitrogen Corp.; Carlsbad, CA). Briefly, the DNA was pipette to PCR-tubes in 2µg aliquots and dH20 was added to a volume of 21µl. 20µl of 2,5x Random Primer Buffer was added and the DNA was denaturized in PCR-machine at 98°C for 5 minutes after which the tubes were moved to ice and 5 µl of 10x dNTP mix, 3 µl of Cy5-dUTP to sample and Cy3-dUTP to reference and 1 µl of Klenow DNA polymerase was added to each tube. The labeling was then carried out in a PCR-machine at 37°C for 2 hours. During labeling the cDNA arrays were pre-treated to prevent DNA from interacting with the glass slide. The empty areas on array located between the cDNA probes were blocked by BSA so that the arrays were incubated in blocking solution containing BSA, SSC and SDS (see Appendix 2). After 30 minute blocking at 50°C the arrays were washed in cuvettes with 2xSSC and 0,2xSSC for 3 minutes each in a shaker and dried by a two minute centrifugation at 400g (Heraeus Multifuge 3s). After the 2h labeling the samples were transferred to eppendor tubes and 5 µl of 0,5M EDTA and 450 µl of TE-buffer pH 7.4 (Biochemika Fluka; Buchs, Switzerland) was added. The unincorporated label was then removed from the solution by centrifuging the samples through Microcon 30 columns (Amicon/Millipore; Bedford, MA). Then the sample and reference DNA was combined into one tube with an addition of human Cot-1 DNA (Invitrogen Corp., Carlsbad, CA), yeast tRNA (Appendix 2), poly dA, poly dT (Amersham Biosciences; Piscataway, NJ) and TE-buffer Ph 7.4. The mixture of labeled reference and tumor DNA was then concentrated using Microcon 30 columns into an exact volume of 48, 56 or 64 µl. The volume was adjusted with dH2O if necessary and to stabilize the solution SSC and SDS was added to a final concentration of 3,4xSSC and 0, 3% SDS. Next the DNA was denaturized in 100°C for 1, 5 minutes and Cot-1 DNA was let to pre-anneal for 30 minutes in 37°C. Coverslip was put on the array and the hybridization solution was pipetted in. The array was then transferred to a hybridization chamber to which drops of 3xSSC had been added to

provide moisture; the chamber was closed tight and put to a water bath set to 65°C. The hybridization was let to happen over night approximately 17h followed by post-hybridization washes in three different solutions 0,5x SSC / 0,1 % SDS 15 min, 0,5xSSC / 0,01 % SDS 15 min, 0,06xSSC 15 min + 2 min (see Appendix 2). To dry the slides a centrifugation (Heraeus Multifuge 3s) in 400 g for 2 minutes was performed. The array used was a 16K Human cDNA microarray containing approximately 16 000 annotated cDNA clones in duplicates (The Finnish DNA Microarray Centre at Turku Centre for Biotechnology).

3.4 cDNA Microarray Data Analysis

Arrays were kindly scanned by Päivi Junni and Marjo Linja at the Finnish DNA Microarray Centre at Turku Centre for Biotechnology with Agilent microarray scanner G2505B (Agilent Technologies; Palo Alto, CA). The results were analyzed using Feature Extraction Software 8.1, GeneSpring 7 (Agilent Technologies; Palo Alto, CA) and aCGH Smooth Programme (freely available software at http://www.few.vu.nl/~vumarray/) (Jong et al., 2004). Chromosomal base-pair localizations of cDNA clones were obtained from the December 2004 freeze of the University of California-Santa Cruz genome browser (http://genome.ucsc.edu/). Feature Extraction Software 8.1 was used to extract the actual fluorescent intensities of each probe on array from the scanned image. Feature Extraction software produces a tab-delimited text file that contains the results from each feature i.e. probe. Information such as gene name, log ratio (base 10), processed signal, mean signal and dye-normalized signal is included. The normalization was done using Lowess normalization. The text file was then inserted into GeneSpring 7 in which the intensities from duplicate probes were averaged, outlier probes were filtered out and the genes were mapped to their chromosomal locations according to data obtained from the December 2004 freeze of the University of California-Santa Cruz genome browser. Outlier probes included probes with intensities over the measurement scale (saturated features) and probes that had an intensity value lower than that measured for the background. The result of GeneSpring 7 was another text file which now contained filtered and located data of probes measured. This text file was

converted in Microsoft Excel to a format required by aCGH Smooth Programme; this included the conversion of intensity ratios to log2 scale. The aCGH Smooth Programme uses a specified algorithm to calculate the breakpoints of chromosome aberrations (Jong et al., 2004). Using the breakpoint information now added to the text file scatter plots displaying both the breakpoints and log2 intensity ratios as a function of genomic Kb location were generated in Microsoft Excel. For each sample a plot representing the whole genome as well as plots representing every chromosome individually was made. The background noise was determined by comparing the scatter plots with the scatter plots of two hybridization controls, the self vs. self hybridization and male vs. female hybridization. At this point four samples were excluded from the study because of high background noise. Furthermore, two samples were left out because University of Valencia provided the clinical data of samples and informed that two of the analyzed samples were not GISTs. Table 4 shows an example of the numerical data included in the text file after final analysis and Figures 14 and 15 display examples of scatter plots.

TABLE 4. Data included in the text file after final analysis. Normalized column comprises the Lowess normalized log10 intensity ratios, common column the common name of cDNA probe and Genebank the genebank ID of probe.

Normalized	Common	Genebank	Map	Chrom	cum bp	Log2Rat	Breakpoint
0.9303432	CXYorf1-related protein	AA485730	1	1	4268	-0.1041651	-0.030851
0.9526693	*pcrmbweak*hypothetical protein MGC45873	R10574	1p36.33	1	919081	-0.0699527	-0.030851
0.9799684	DKFZP564C186 protein	AA427857	1p36.33	1	919718	-0.0291929	-0.030851
0.9492135	DKFZP564C186 protein	AA026278	1p36.33	1	919738	-0.0751956	-0.030851
0.7941176	interferon, alpha-inducible protein (clone IFI-15K)	AA406020	1p36.33	1	989514	-0.3325754	-0.030851
1.0024345	calcium binding protein Cab45 precursor	AI129590	1p36.33	1	1193841	0.003508	-0.030851
0.8334584	sodium channel, nonvoltage-gated 1, delta	AI361695	1p36.3-p36.2	1	1266677	-0.2628179	-0.030851
1.0332903	*pcrmbonestrong*centaurin, beta 5	W74261	1	1	1267692	0.0472456	-0.030851
0.9225847	centaurin, beta 5	R49810	1	1	1278224	-0.1162468	-0.030851
0.9082032	hypothetical protein FLJ20542	AA991426	1p36.33	1	1286904	-0.1389129	-0.030851

cDNA microarray result sample 32 whole genome
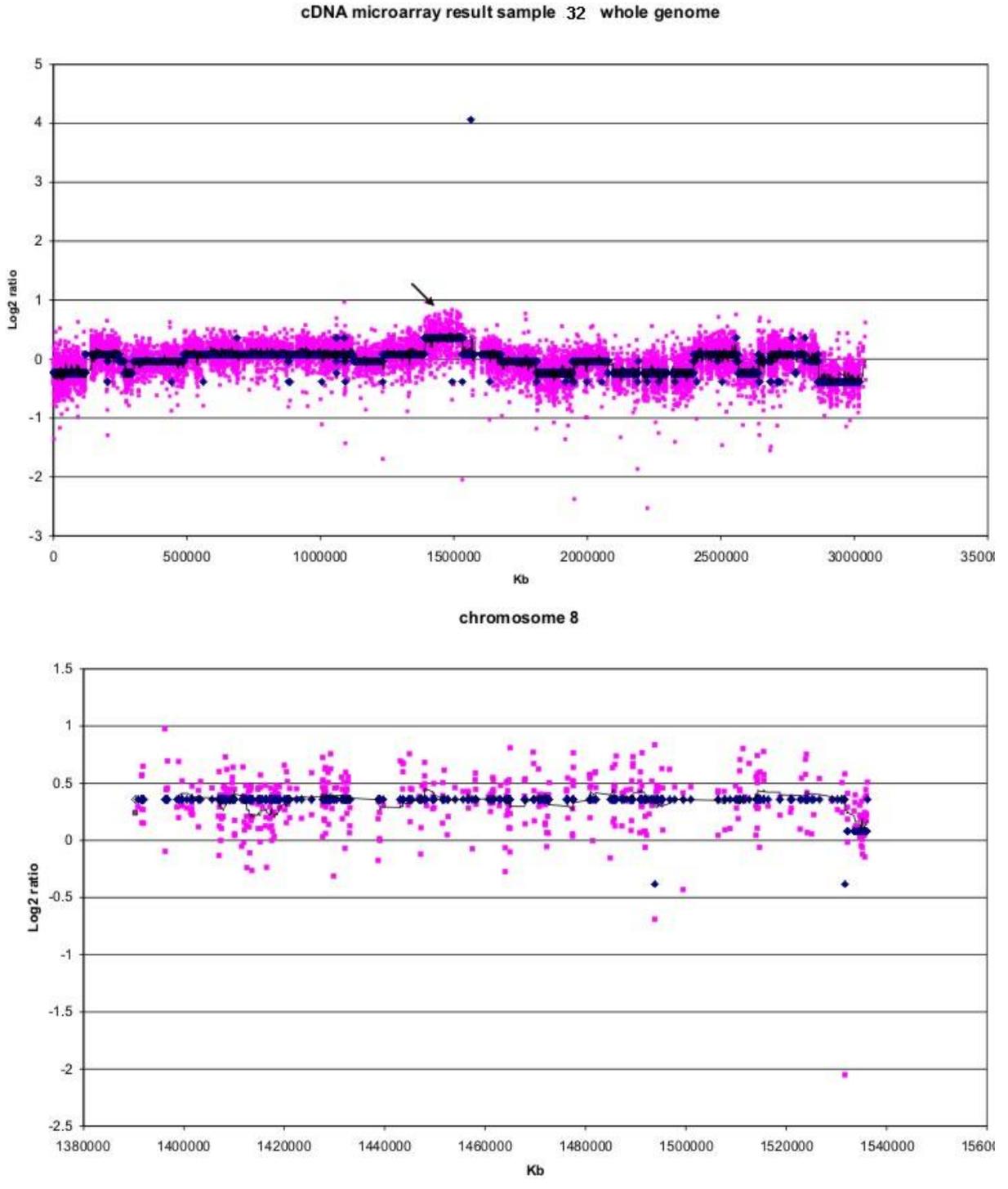

chromosome 8

FIGURE 14. A whole genome scatter plot showing many copy number changes. Copy number gain at chromosome 8 is pointed by an arrow and the individual scatter plot is shown below.

**sel vs. self control**

male vs. female control
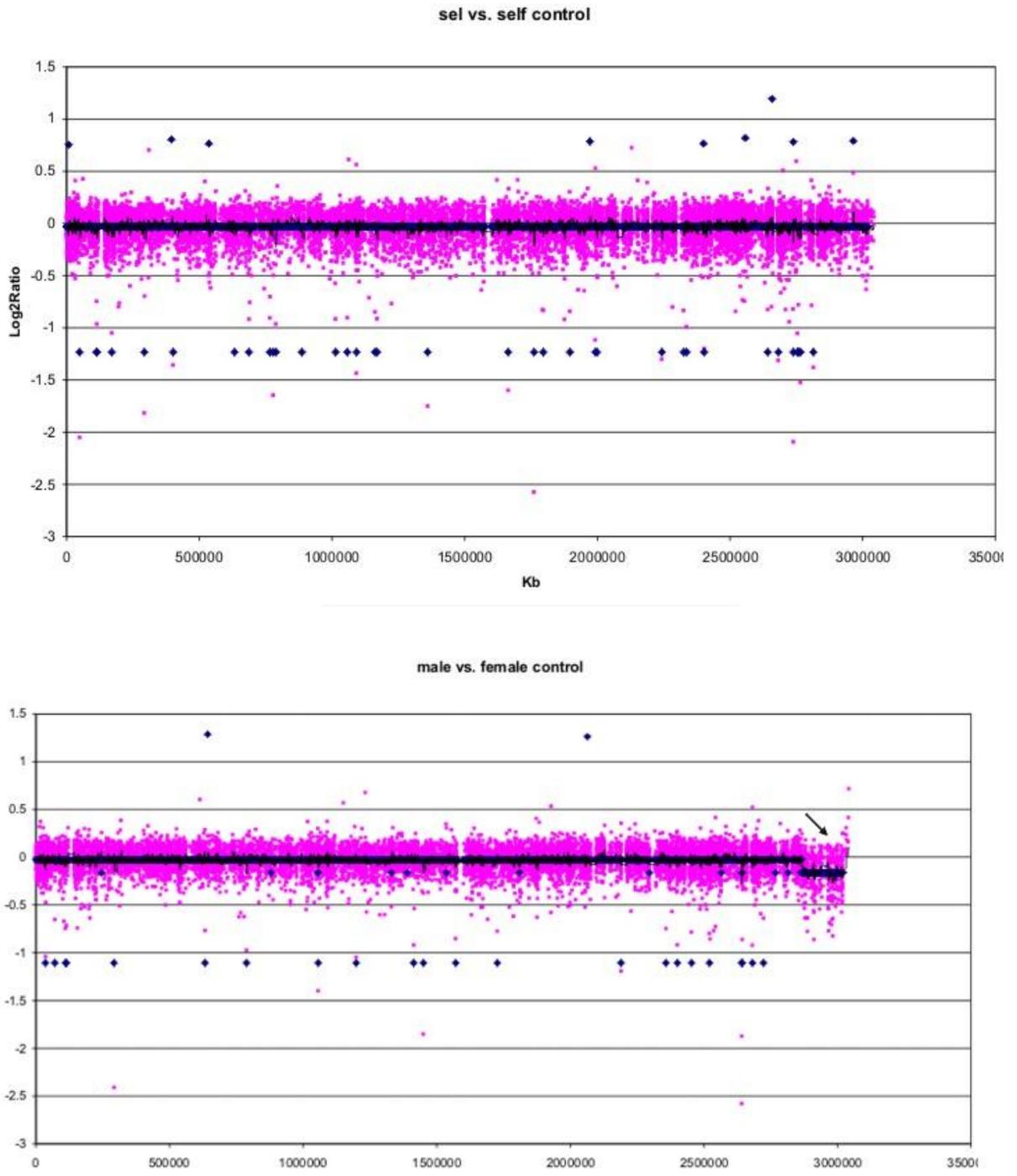
FIGURE 15. The background noise was approximated from the control hybridizations displayed above. The arrow points to X chromosome.

From the scatter blots a general view of chromosomal imbalances was seen. Next those chromosomes that had aberrations were investigated in more detail. The length of aberration, the starting and end point and the number of probes included were looked from the numerical data of final text file. All aberrations that included five or more probes were taken into account and listed on a separate file sample by sample as demonstrated in Table 5.

TABLE 5. An example of data gathered from the text file after final data analysis.

Sample	Losses	start site kb	end site kb	probes	Size Mb
GIST no.2	1p36.22 - 1p36.33	4.268	9844.433	69	9.840165
	3p25.2 - 3p26.3	487854.46	500974.55	52	13.12009
	3p24.1 - 3q11.2	516889.26	583615.72	274	66.726462
	8p12 - 8p23.3	1389529.6	1420079.9	121	30.550308
	14q32.33 - 14q11.2(whole chrom)	2191028.7	2296474	416	105.44538
	19q13.12 - 19q13.2	2682431.3	2684943	17	2.511726
	19q13.2	2686942.9	2688038	10	1.095038
	21q22.3 - 21p11.2(whole chrom)	2767664.6	2814665.8	138	47.001269
	Gains	start site kb	end site kb	probes	Size Mb
	1q25.3 - 1q44	179944.88	245353.05	291	65.408169
	3p24.1 - 3p25.2	501140.54	516889.26	54	15.748723
	3q26.1 - 3q29	657425.48	687707.49	138	30.282011
	8p11.21 - 8p12	1420401.1	1430427.9	40	10.026777
	8q21.12 - 8q24.3	1469599.4	1531657.4	150	62.057996
	17q23.2 - 17q25.1	2543992.1	2557359.8	82	13.367638
	18q23	2640781.9	2641390.9	7	0.608936
Sample	Losses	start site kb	end site kb	probes	Size Mb
GIST no.20	1q12 - 1p36.33	4.268	142560.57	779	142.5563
	5p15.2 - 5p15.33	879295.34	890483.93	30	11.188588
	13q34 - 13p13(whole chrom)	2077021.8	2190995.5	281	113.97371
	14q11.2 - 14q21.1	2210952.6	2229970.7	122	19.01816
	15q11.2 - 15q26.3(whole chrom)	2316076.2	2397450.8	401	81.374581
	21p11.2 - 21q22.3(whole chrom)	2767664.6	2814662.2	146	46.997622
	22p13 - 22q13.33(whole chrom)	2814719.3	2864199.7	315	49.480428
	Gains	start site kb	end site kb	probes	Size Mb
	3q25.2 - 3q29	644017.23	687618.01	179	43.600772
	8p23.3 - 8q24.3(whole chrom)	1390322.8	1536046.3	475	145.72348
	9p21.1 - 9p24.3	1536305.7	1568738.3	67	32.432599
	16p12.3 - 16p13.3	2397827.2	2417566.4	172	19.739242

When all 35 samples were analyzed the minimal common overlapping areas of copy number imbalances were recorded by aligning all aberrations chromosome by chromosome in an ideogram as demonstrated in Figure 16.
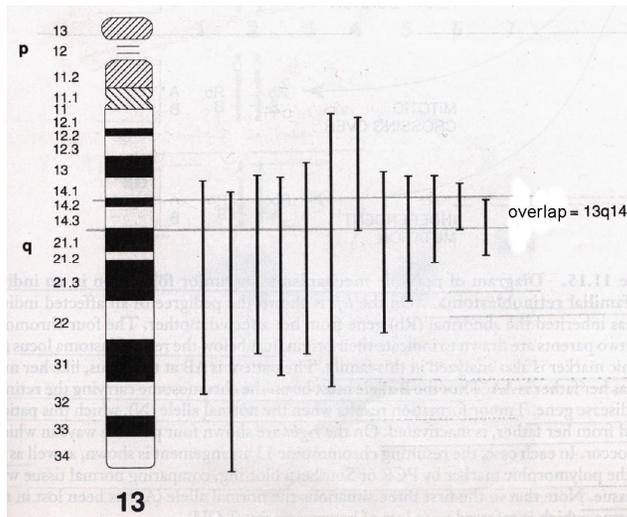
FIGURE 16. Schematic presentation of the identification of minimal common overlapping areas. The area is defined as the region between the furthest start of aberration and the earliest end of aberration. (Thomas et al., 1998)

Finally the location, starting and end point, size and number of actual genes in the overlapping areas were recorded. This was done with the help of Ensembl project (http://www.ensembl.org/index.html) and GeneCards^{TM} integrated database (http://www.genecards.org/) so that the gene corresponding to the first and last probe of copy number imbalance was searched using these services and the gene data concerning the region between these two genes was exported from Ensembl. This way the amount of actual genes identified in the region was obtained. There was a discrepancy between the kb locations of Ensembl and cDNA array because the genomic map locations of cDNA probes were derived by using a cumulative base pair identifier whereas Ensembl uses individual kb locations for each chromosome. Both kb locations were recorded but the Ensembl one was used in the final results. An example of data gathered is displayed in Table 6.

TABLE 6. An example of data gathered from the minimal common overlapping areas of copy number imbalance.

location	overlapping area kb (cDNAarray)		overlapping area bp (Ensembl)		size of area Mb calculated from cDNAarray bp	number of genes in area according to Ensembl	occurs in x/35 samples
Losses:							
1p36.22 - 1p36.23	8007.418 9844.433	-	8051572 9904548	-	1.8	43	24
1p35.1 - 1p35.3	28647.102 32178.191	-	28664604 32195543	-	3.5	82	19
1q21.2 - 1q22	146670.559 152102.473	-	146541344 152104408	-	5.4	376	4
1q44	245314.398 245353.957		245314402 245363035	-	0.04	6	5
2p16.3 - 2p24.1	265677.326 294331.361	-	20154041 48894468	-	28.6	464	3
2p11.2 - 2q11.1	334257.093 341021.026	-	88830461 95713309	-	6.8	84	3
3p21.31	538907.243 539937.064		50367184 50979344	-	1	17	6
3p25.2 - 3p26.3	487954.763 500974.546	-	826977 12450847	-	13	165	2

The minimal common overlapping areas provided a good overview of recurrent copy number imbalances in GISTs and represented important data as such. However, the aim was also to identify some of the target genes of chromosomal imbalances and therefore the gene lists provided by Ensembl were investigated. Genes involved in gene repair, cell cycle control and tumor suppression were screened for in areas of copy number loss and oncogenes and genes involved in cell proliferation were screened for in areas of copy number gain. Only areas with a reasonable number of genes (less than 100) were screened. Genes that had been implicated in previous GIST publications were emphasized and if an interesting gene appeared in the Ensembl gene list the intensity ratio of corresponding cDNA probe was observed from all samples in the overlapping area. To conclude it can be said that the data analysis of cDNA arrays was somewhat tedious but it did eventually allow identification of some target genes of chromosomal imbalances.

3.5 Labeling and Hybridization Oligoarray

To confirm the results of cDNA array eight individual samples were replicated on a higher resolution 60-mer oligonucleotide-based microarray namely the 44K CGH miroarray (Agilent Technologies; Palo Alto, CA) which contains approximately 43 000 probes sourced and mapped from the NCBI genome Build 35. For oligoarray 1.5 μg of both reference and tumor DNA was labeled as before now using the BioPrime Plus Array CGH Genomic Labeling Kit (Invitrogen Corp.; Carlsbad, CA). The labeled DNA was mixed and hybridized to array using Human Genome CGH Microarray Kit 44B (Agilent Technologies; Palo Alto, CA) according to the manufacturer's protocol. Briefly, human Cot-1 DNA (Invitrogen Corp.; Carlsbad, CA), Agilent 10xBlocking Agent and Agilent 2xHybridization Buffer were added to the labeled sample mixtures. The DNA was then denaturized in 95°C water bath for 5 minutes after which the Cot-1 DNA was let to pre-anneal for 30 minutes in 37°C. Agilent SureHyb chamber base was loaded with a gasket slide, the sample and array were added and the chamber was taken to a rotating hybridization oven se to 65°C. After 40h hybridization the arrays were washed according to manufacturer's wash procedure B (without stabilization and drying solution) so that the hybridization chambers were disassembled immersed in Agilent Wash Buffer 1 and the arrays washed in slide staining dishes filled first with Agilent Wash Buffer 1 at room temperature for 5 minutes and second for one minute with Agilent Wash Buffer 2 that had been pre-warmed to 37°C the previous day.

3.6 Oligoarray Data Analysis

Arrays were scanned at Biomedicum Biochip Center with Agilent microarray scanner G2565BA and analyzed with Feature Extraction Software 8.1 and CGH Analytics software 3.2 (Agilent Technologies; Palo Alto, CA). CGH Analytics software 3.2 allowed simultaneous data filtering, chromosomal mapping, breakpoint identification and result visualization inside one programme. It also enabled gene-level investigation of the aberrations identified. An example of CGH Analytics result images is displayed in Figure 17.
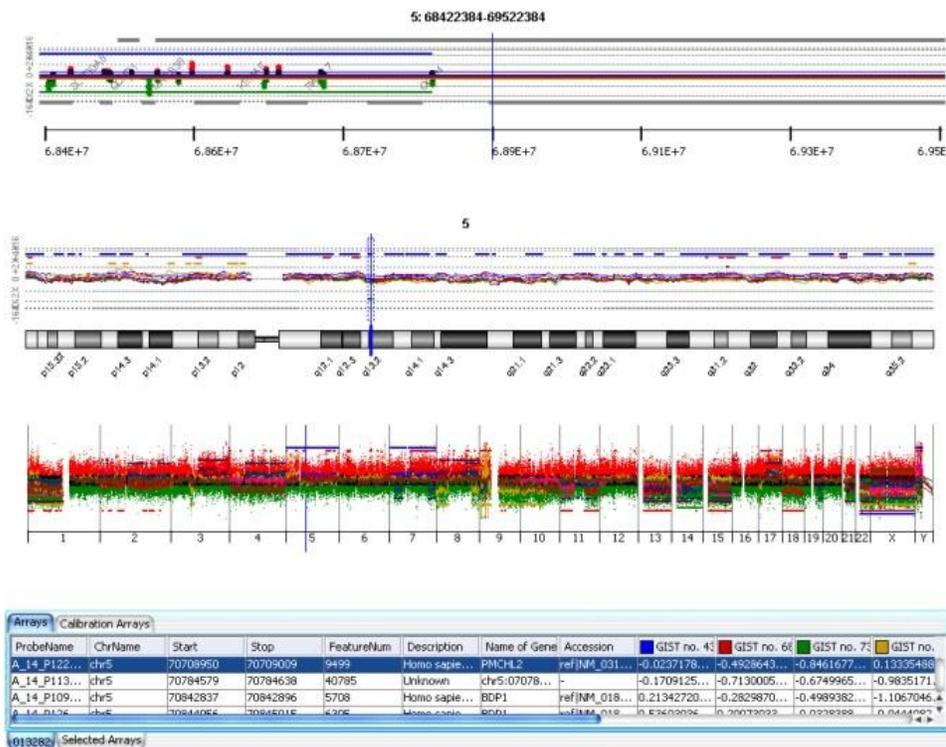
FIGURE 17. Result visualization in CGHAnalytics. Reading from up the gene view shows the oligo probes and names of the corresponding genes, chromosome view shows the imbalances in a chromosome and the genome view shows imbalances in the whole genome.

3.7 Control Hybridizations

Two control arrays were used in the experiment. A self vs. self hybridization was carried out using male reference DNA so that the same DNA was labeled with both Cy3 and Cy5. A male vs. female array was also made using the reference DNA so that male DNA was labeled with Cy5 and female DNA with Cy3. The results of control arrays were used to approximate the level of noise on sample hybridizations. For oligoarrays quality control was done with the help of QC Metrics tool in CGH Analytics Programme (Agilent Technologies; Palo Alto, CA). In the analysis of oligoarray results control arrays were performed as before and used as calibration arrays on CGH Analytics.

4. Results

All samples were first screened for chromosomal imbalances by cDNA microarrays with results represented at Figure 18. The minimal common overlapping areas of copy number imbalances are represented in Table 7.
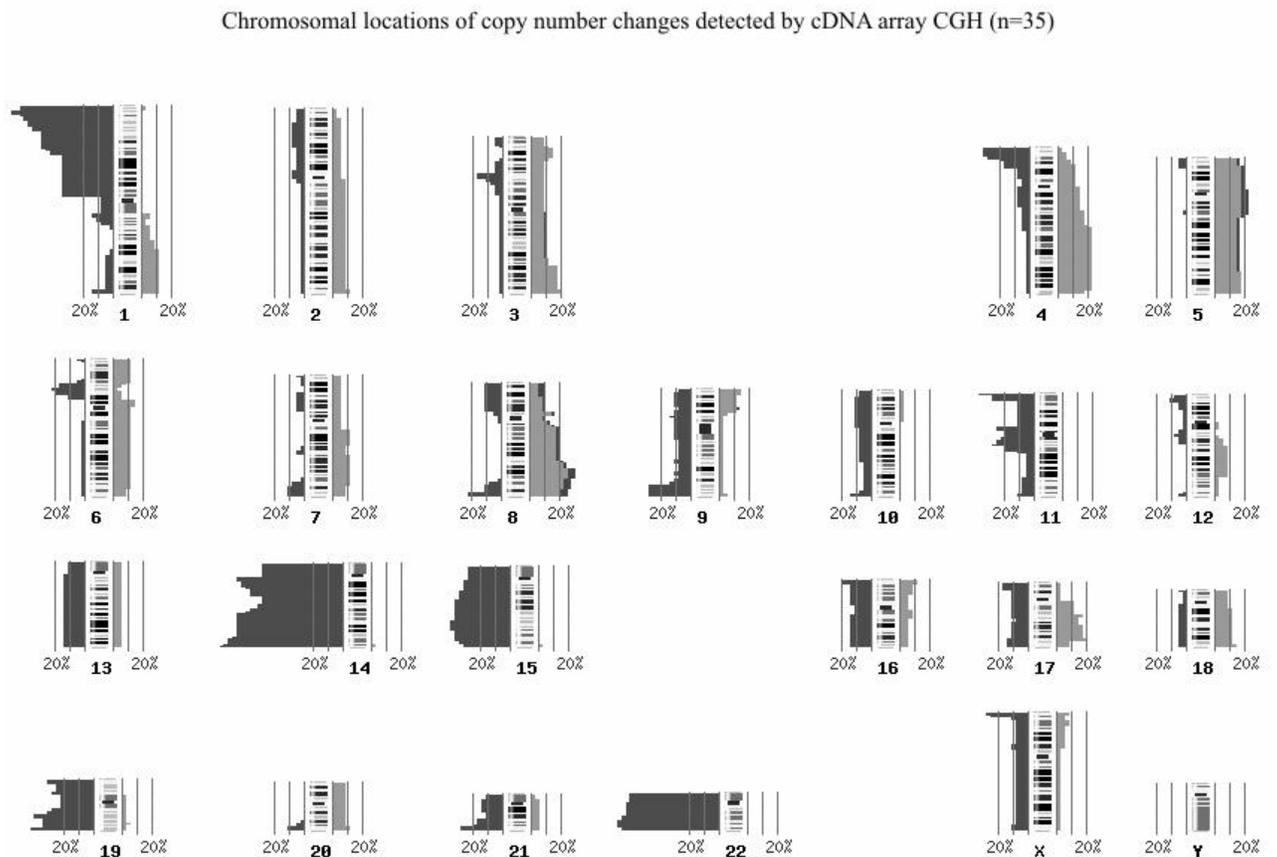
FIGURE 18. Copy number imbalances and their frequency as found in the current study. Losses (dark grey bars) are displayed on the left and gains (light grey bars) on the right hand side. Chromosomal ideograms were generated with software from the PROGENETIX http://www.progenetix.net project. (Baudis and Cleary, 2001)

TABLE 7. Minimal common overlapping areas of detected copy number losses and gains by cDNA array CGH.

DNA copy number losses:				
chromosomal location	overlapping area bp location	size of area Mb	number of genes in area	aberration present in no. samples n=35
1p36.22 - p36.23	8051572 - 9904548	1.8	43	24
1p35.1 - p35.3	28664604 - 32195543	3.5	82	19
1q21.2 - q22	146541344 - 152104408	5.4	376	4
1q44	245314402 - 245363035	0.04	6	5
2p16.3 - p24.1	20154041 - 48894468	28.6	464	3
2p11.2 - q11.1	88830461 - 95713309	6.8	84	3
3p21.31	50367184 - 50979344	1	17	6
3p25.2 - p26.3	826977 - 12450847	13	165	2
4p15.33 - p16.3	665619 - 11092053	10.4	212	11
4q35.2	191005794 - 191259507	1.2	4	2
5p15.2 - p15.33	324739 - 11080418	10.7	101	2
6p25.3	336760 - 1557341	1.3	15	2
6p21.31 - p21.33	30212487 - 35546536	5.4	300	9
7p22.3	645370 - 2247455	1.6	49	2
7p13 - p15.3	23112200 - 43438962	20.5	251	2
7q22.1	99335055 - 101851111	2.4	144	2
7q35 - q36.3	145251617 -158121795	10.5	215	4
8p12 - p23.3	431647 - 30160601	29.8	416	4
8q24.3	142387234 - 146097650	3.8	164	8
9p21.3 - p24.1	5909023 - 21999312	16.1	143	4
9p13.2 - q12	36204441 - 65814005	31.8	147	4
9q33.3 - q34.3	127239017 - 136716075	9.4	367	11
10p15.3 - 1q11.21	82997 - 42945105	42.7	592	4
10q26.3	133632018 - 135241501	1.6	52	4
11p15.5	192926-2907226	2.7	149	13
11p11.2	45783217 - 47308158	1.5	45	9
11q13.2	65869420 - 67047475	1.1	79	10
11q25	131286586 - 133787022	2.5	22	4
12p13.31	6326276 - 7202795	0.9	83	4
12q13.13 - q13.2	49774889 - 54634072	3.6	205	4
12q24.33	131955845 - 132074548	0.09	9	2
13q	whole q arm			5
14q11.2	19881071 - 23680634	3.8	218	26
14q32.33	104246060 - 105188441	0.9	87	30
15q23 - q25.1	70197808 - 79403579	9.3	220	14
16p13.3	74273 - 2590978	2.5	240	8
17p13.3	608938 - 1366719	0.7	21	6
17q25.1 - q25.3	70642938 - 78039430	7.8	298	5
19p13.3	367593 - 568157	0.2	14	11
19p13.11	18252251 - 18409977	0.2	13	10
19q13.2	45413807 - 46581825	1.1	74	13
19q13.43	63679564 - 63802660	0.1	13	14
20q13.33	61689399 - 62338320	0.6	63	4

21q22.3	43267712 - 46428729	3.1	111	11
22q13.1 - q13.31	38222784 - 43901242	5.7	215	24
Xp22.33	160025 - 2652702	2.5	36	8
Xp22.31 - p22.33	2740357 - 8509963	5.5	44	6

DNA copy number gains:

chromosomal location	overlapping area bp location	size of area Mb	number of genes in area	aberration present in no. samples n=35
1q31.2 - q32.1	189879833 - 202022540	12.1	201	3
2q37.3	241765505 - 242346217	0.5	20	5
3q29	198849260 - 198952015	0.2	3	7
3p24.1 - p25.2	12629892 - 30710628	18.1	151	6
4q23 - q35.2	101226420 - 188020136	86.8	900	9
5p15.2 - q13.2	14634932 - 72897254	58.3	580	7
6p22.1 - p25.3	336760 - 29966825	29.7	521	4
6p12.1 - p12.2	52869404 - 57506276	4.8	72	5
6p12.2 - q25.3	52869404 - 160189871	107	1255	4
7q11.23 - q21.3	75043503 - 96415608	21.4	279	4
7q22.1 - q34	101983606 - 141912568	40	641	4
8p11.21 - p12	30361585 - 40131599	10	137	5
8q23.2 - q24.13	111048411 - 124423903	13.3	92	11
9p24.1 - p24.3	111039 - 5823070	5.7	92	5
9p21.2	26830685 - 27516491	0.5	14	4
12q15 - q23.3	69201231 - 106608724	37.4	381	3
13q	whole q arm			2
16p13.3	36405 - 3667061	3.6	339	4
16q11.2 - q12.1	45251095 - 46096935	1	21	4
17q21.31	38430891 - 40493912	2	123	5
17q23.2	53786039 - 55325078	1.5	50	6
17q25.1	70780669 - 71611406	0.8	47	4
18q23	75502974 - 75999217	0.6	12	5
19q13.33	54309430 - 55560743	1.2	100	2
20	whole chromosome			3

The individual results of all 35 samples are displayed in appendix 3. Most common losses were located at 14q, 22q and 1p. Gains were most recurrent at 8q. Figure 19 displays the frequency of aberrations in each chromosome.
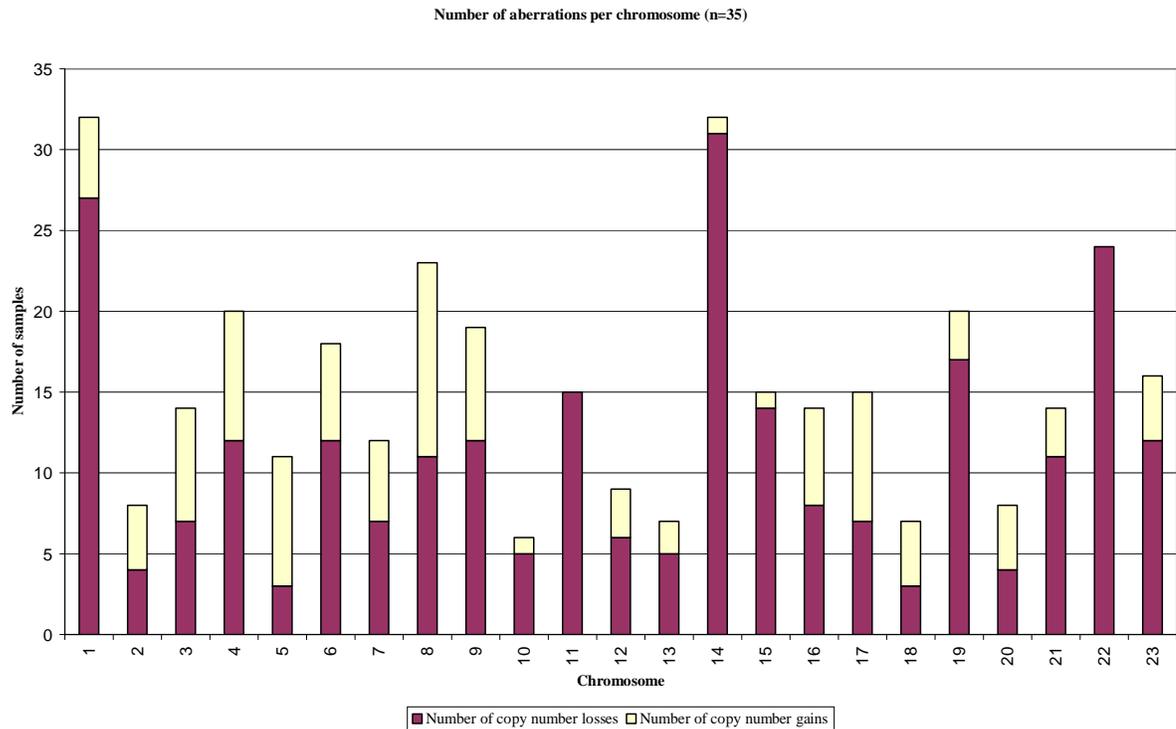
FIGURE 19. Chromosomal imbalances and their frequency in each chromosome.

The results revealed two minimal common overlapping areas at chromosome 14, one at 14q11.2 and another at 14q32.33. Copy number imbalance on 14q was especially frequent and only four samples had no copy number loss at 14q. To confirm these results eight samples were selected for further analysis and confirmation of results with parallel oligoarray hybridizations. Copy number loss at 14q was the most frequent finding in the current sample series. All of the benign tumors and 80% (16/20) of malignant tumors had a loss in 14q. Overall 31 samples (~ 89%) represented this loss with more than half of samples (19/31) having a loss of whole q-arm. Only three samples had a normal chromosome 14 and one sample had a minor copy number gain on q-arm. Interestingly 12 samples had either one or two distinct sites of copy number losses at either proximal or distal part of chromosome 14. The loss was proximal in seven and distal in five of these samples. Furthermore, six samples featured both proximal and distal copy number loss interrupted with varying length of normal sequence. Consequently the minimal common overlapping areas were mapped to 14q11.2 representing the proximal loss and to 14q32.33 representing the distal loss.

The 14q11.2 location identified by cDNA array covered approximately 200 genes and therefore three samples representing the loss were hybridized on oligoarray. The expectation was to confirm the presence of an overlapping area at 14q11.2 and to identify a smaller list of target genes. The results showed one sample with normal chromosome 14, one with a larger proximal loss at 14q11.2-q23.3 and one with a loss of 14q11.2. When all eight replicate oligoarrays were aligned a common overlapping copy number loss at 14q11.2 was defined as seen in Figure 20.
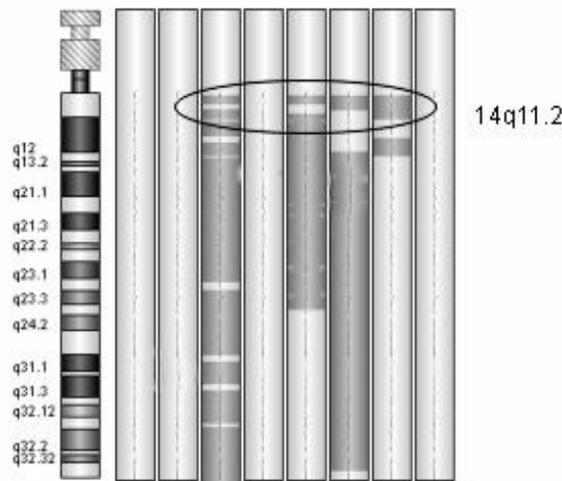
FIGURE 20. The minimal common overlapping area of copy number loss at 14q11.2 as verified by oligoarray experiment.

Furthermore, the established area was small enough to allow gene-level investigation. As a result the oligoarray experiment confirmed overlapping area at 14q11.2 and allowed identification of three possible target genes involved in DNA repair and tumor suppression; *PARP2, APEX1* and *NDRG2*. The cDNA array data on 14q32.33 revealed one interesting gene representing a copy number loss. This gene, *SIVA* is a protein coding gene involved in the apoptotic pathway induced by CD27 antigen. It is a good candidate gene for the target of copy number loss at 14q32.33. Unfortunately out of the five oligoarray replicated samples representing this distal 14q copy number loss only one showed a separate distal deletion and

the rest had either the loss of whole q-arm, normal chromosome 14 or proximal loss at 14q11.2. The sample with a separate distal deletion had both a proximal loss at 14q11.2 and a distal loss at 14q31.1-q32.33. However, the distal loss comprised a much larger area than that shown on cDNA array. Thus the presence of an overlapping area at 14q32.33 was not confirmed by parallel oligoarray experiments and the importance of this location in relation to GIST pathogenesis requires further investigation. In addition the oligoarray experiment included two malignant tumors that on cDNA array showed a normal chromosome 14. We hypothesized that these tumors might have smaller losses not detected by cDNA array but detectable on a higher resolution oligoarray. The results did not support hypothesis, both tumors illustrated a normal chromosome 14 on oligoarray as well.

In 9p the minimal common overlapping areas of chromosomal aberrations detected by cDNA array form an interesting pattern in which a deleted area is located in between two gains as seen in Figure 21.
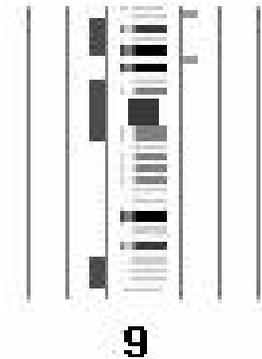
FIGURE 21. Chromosome 9 minimal common overlapping areas of aberrations detected by cDNA array CGH. Losses (dark grey bars) are displayed on the left and gains (light grey bars) on the right hand side. A pattern of copy number loss flanked by two copy number gains in the p-arm is illustrated. Chromosomal ideogram was generated with software from the PROGENETIX http://www.progenetix.net project. (Baudis and Cleary, 2001)

When the results of both arrays were further investigated it was found that in fact the loss of 9p is seen in six samples and in three of them the breakpoint of aberration is located at 9p21.3 the locus of *CDKN2A/2B* genes. Four samples displayed a copy number loss of *CDKN2B* printed on cDNA array. Oligoarray included probes for both *CDKN2A/2B* genes and additional two samples displayed a loss of these genes as detected on oligoarray only. Interestingly in

one sample the aberration occurs at a breakpoint of a loss and gain and this is seen on both arrays as displayed at Figure 22.
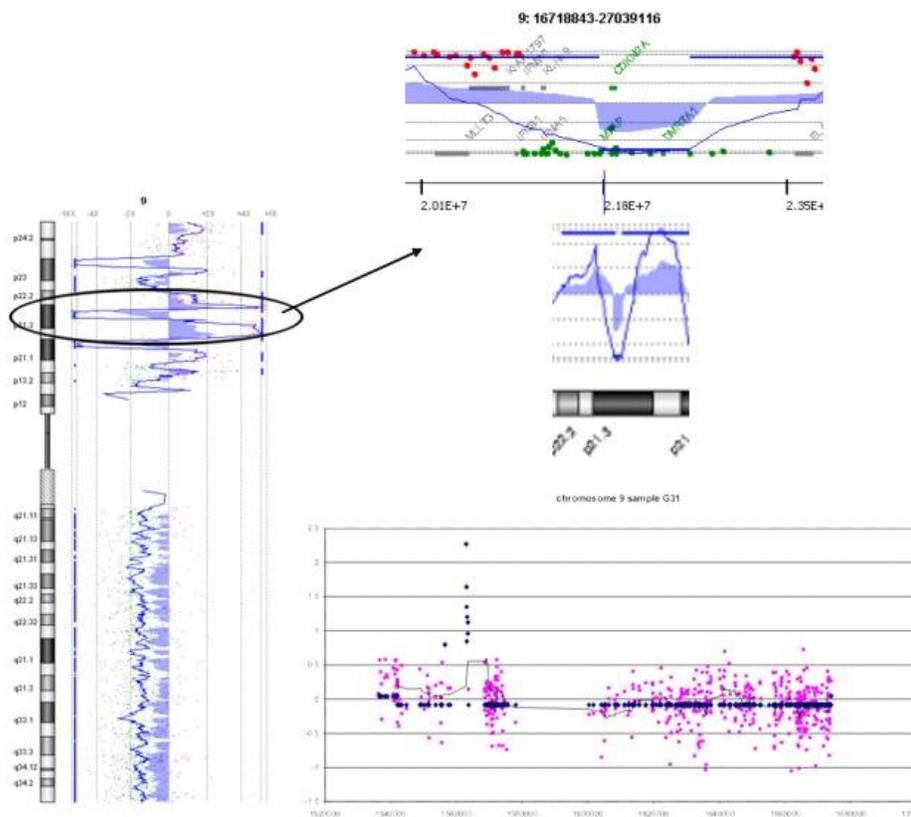
FIGURE 22. Chromosome 9 of sample GIST no. 31 as seen on oligoarray (upper pictures) and cDNA array (lower picture). cDNA array shows a copy number loss of lower magnitude than that seen on oligoarray, also the two gains are merged into one in cDNA array.

Moreover in current sample series the loss of 9p is seen almost exclusively in malignant tumors, five out of the six tumors displaying 9p loss are malignant. Chromosomal aberrations in chromosome 1 were also frequent and as a result four minimal common overlapping areas were located. The most recurrent area mapped to 1p36.22 - p36.23 and included a copy number loss of *ENO1* a protein coding gene for one of the enolase isoenzymes. There is a loss in 1p in 13 out of the 15 benign samples (~ 87%) and in 15 out of 20 malignant samples (75%) thus the current results do not link 1p loss with malignancy but rather suggest it is an early change in GIST pathogenesis. Chromosome 8 on the other hand was found as a recurrent gain especially in malignant tumors. The minimal common overlapping area of copy number gain

at 8q23.2 - q24.13 includes the *MYC* proto-oncogene and this gene was found as a copy number gain in 11 samples. The presence of a gain in 8q is related to malignancy with 55% (11/20) of malignant samples displaying it. Also 4 benign samples featured a gain in 8q.

The cDNA clone of *NF2* is printed on the array and thus has a copy number loss in all of the 21 samples representing a loss of whole chromosome 22. *NF2* is also deleted in one sample having two separate losses one at 22q11.1-q13.1 and another at 22q13.1-q13.33. The first deletion contains *NF2*. Overall 60% (9 /15) of benign samples and 75% (15 /20) of malignant samples contained losses at 22q. Copy number gains in chromosome 4 were detected in 8 samples. Interestingly five of these tumors have the *KIT* gene at 4q12 gained. However, in each case the gained area is not restricted to 4q12 but comprises the whole q arm. The minimal common overlapping area is also located outside the *KIT* locus indicating that despite the detected copy number gain of *KIT* it might not be the actual target gene of this aberration. Yet according to these results *KIT* is represented as a copy number gain in a subset of GISTs. Mutation analysis was completed in only one of the samples displaying *KIT* gain and exon 11 mutation, there is no follow up data from this benign sample but the current status of the patient is dead. Chromosome 12 also featured some interesting copy number gains. Three samples embodied gains in chromosome 12 with a minimal common overlapping region mapped to 12q15 - q23.3. This region comprises a known oncogene *MDM2*. Two samples displayed a copy number gain of *MDM2* located at 12q15, a breakpoint of the aberration.

To conclude, the results of current study provide an overview of chromosomal aberrations in gastrointestinal stromal tumors displayed by the minimal common overlapping areas. In chromosome 14 an area of recurrent copy number imbalance was established at 14q11.2 and *PARP2, APEX1* and *NDRG2* genes are suggested as possible target genes. They might be underlying the development of GIST. Another area at 14q32.33 comprising the locus of *SIVA* was also identified but as it could not be confirmed by parallel oligoarray hybridizations further research is required to establish the recurrence of this chromosomal imbalance. As perhaps the most interesting outcome concerning the gene-level investigation a loss of *ENO1* at 1p36.23 and a gain of *MYC* at 8q was identified. A summary of relevant genes found as a copy number loss or gain as a result of present study is provided in Figure 23.

A. Summary of genes found as a copy number loss

1p36.23
ENO1

9p21.3
CDKN2A/2B

14q11.2
PARP2
APEX1
NDRG2

14q32.33
SIVA

22q12.2
NF2

B. Summary of genes found as a copy number gain


4q12
KIT

8q24.12-q24.13
MYC

12q15
MDM2
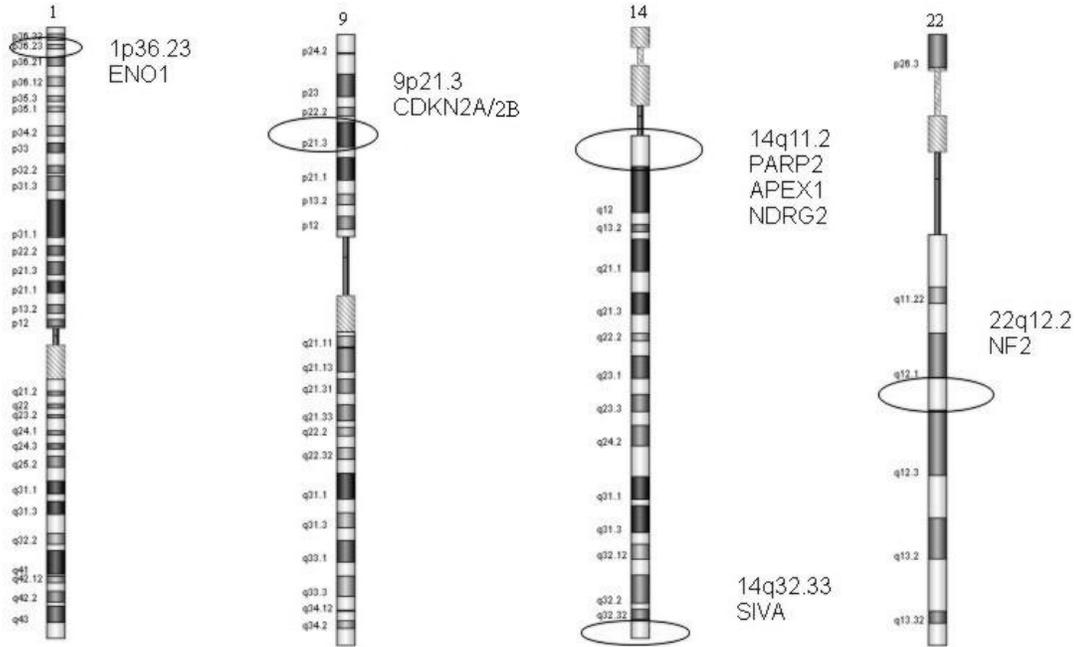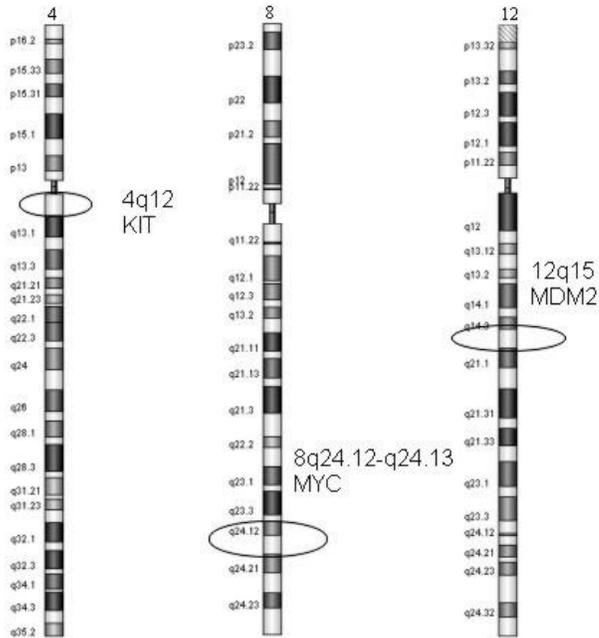
FIGURE 23. Summary of target genes identified as a copy number loss (A) or gain (B) at the site of chromosomal imbalamce.

5. Discussion

GIST is a stromal tumor of the gastrointestinal tract usually representing a noncomplex cytogenetic profile with certain chromosomal aberrations that distinguish them from leiomyomas and leiomyosarcomas. Yet the molecular pathogenesis and the target genes of chromosomal rearrangements of this tumor are poorly understood. The findings of present study confirm some of the earlier results derived from LOH and cCGH studies and propose new candidate genes that could have a role in the molecular pathogenesis of GISTs. Loss of DNA copy number in 14q is the most recurrent cytogenetic change in GISTs, and has been reported in approximately equal proportions in benign and malignant GISTs. It is therefore thought to be an early event in GIST development following *c-KIT* mutation (Breiner et al., 2000; Chen et al., 2004; el-Rifai et al., 1996). The minimal common overlapping regions of loss have been identified to 14q11-q12 and 14q23-q24.3 by El-Rifai et al. and further to 14q11-q12, 14q22-q23 and 14q24.3 by Debiec-Rychter et al. It has been suggested that tumor suppressors and/or gene repair genes located in these regions may be involved in the pathogenesis of GIST (Debiec-Rychter et al., 2001b; El-Rifai et al., 2000b). Other frequent genetic alterations reported have been the loss of 22q and 1p. Involvement of neurofibromatosis 2 (*NF2*) tumor suppressor gene in conjunction with 22q loss has been argued (Fukasawa et al., 2000; Lasota et al., 2005; Pylkkanen et al., 2003). Furthermore, presence of a tumor suppressor at 1p36 and the linkage of malignancy and 1p loss have been reported (Gunawan et al., 2002; O'Leary et al., 1999). In addition the loss of 9p in relation to malignancy and the involvement of p16^{INK4A} gene have been recently investigated. Gene and protein expression studies show that p16^{INK4A} is not expressed in malignant GISTs indicating that it might be a target gene for the loss of 9p21 (Kim et al., 2000; Perrone et al., 2005; Sabah et al., 2004). Also amplification of *c-KIT* locus at 4q12 as a complimentary mechanism of KIT activation has been studied (Tabone et al., 2005).

The most frequent copy number aberrations of present study were the losses located at 14q, 22q and 1p. The loss at 14q was frequent in both benign and malignant tumors. These results confirm the findings of previous reports (Knuutila et al., 1998; Sarlomo-Rikala et al., 1998a; Chen et al., 2004). No tumor suppressor genes have been identified to 14q however

recent studies on other human cancers indicate 14q32 as a possible site for tumor suppressors. Two molecular genetics studies on other neoplasm of digestive tract did in fact map this region as a target for genes responsible for the malignancies of these cancers (Dai et al., 2005; Ko et al., 2005). Moreover 14q32 was most frequent aberration found in GIST by one study that used FISH-probes (Debiec-Rychter et al., 2001a). The candidate gene identified at 14q32.33 in the current study is *SIVA* which appears to have an important role in the regulation of apoptosis. SIVA protein binds to CD27 which is a member of TNFR (tumor necrosis factor receptor) superfamily. The protein complex formed by the binding of SIVA has been shown to induce apoptosis in cell lines (Prasad et al., 1997). The function of *SIVA* supports the suggestion that it might be a target of the copy number loss at 14q32. Unfortunately we were unable to confirm the overlapping area at 14q32.33 and thus further studies are needed to assess both the aberration location and involvement of *SIVA*. The minimal common overlapping region of loss at 14q11.2 identified in this study is consistent with earlier studies reporting recurrent area at 14q11-q12 (Debiec-Rychter et al., 2001b; El-Rifai et al., 2000b). The result of current study define this area more precisely providing new information on the location of copy number loss. The small size of aberrant area at 14q11.2 together with a powerful array based method allowed us to identify three possible target genes *PARP2, APEX1* and *NDRG2*. *PARP2* encodes a nuclear protein which functions in response to DNA strand break having a role in DNA repair, regulation of apoptosis, and maintenance of genomic stability (Johansson, 1999). *APEX1* is another DNA repair enzyme; it has a role in the repair mechanism of AP sites which are pre-mutagenic lesions that can prevent normal DNA replication (Robson and Hickson, 1991). The involvement of *APEX1* in the copy number deletions of 14q was first suggested by El-Rifai et al. in 2000 (El-Rifai et al., 2000b). *NDRG2* belongs to N-myc down regulated gene family. It is a candidate tumor suppressor gene implicated in liver, brain and central nervous system tumors (Deng et al., 2003; Hu et al., 2004; Lusis et al., 2005; Okuda and Kondoh, 1999). As a result the present study confirms the copy number loss of *APEX1* in GIST as directly measured by array CGH and proposes that *PARP2* and *NDRG2* also play a role in the development of GIST. In this study two malignant tumors displayed a normal chromosome 14 whereas all the benign tumors had a loss in 14q. This supports earlier reports stating that the loss of 14q is important especially in the

development of GIST and suggests that other cytogenetic changes are responsible for the progression of tumorigenesis (Breiner et al., 2000; Chen et al., 2004; el-Rifai et al., 1996).

The loss of 9p and the breakpoint of aberration at 9p21.3 found in the present study are rather interesting because of the *CDKN2A/2B* genes located at the breakpoint. *CDKN2A* codes for two key tumor suppressor proteins p16^{INK4a} and p14^{ARF} involved in the regulation of cell cycle G1 and G2/M control. *CDKN2B* codes for a p16-related cyclin-dependent kinase inhibitor p15^{INK4b}. Together these three tumor suppressors regulate two important checkpoints of cell cycle and the loss of these genes can lead to replicate senescence, cell immortalization, and tumor generation (Enders, 2003; Hannon and Beach, 1994; Kamb et al., 1994; Serrano et al., 1993). The role of p16^{INK4a} protein in the carcinogenesis of GIST has been studied earlier. The results link p16^{INK4a} loss to poor prognosis and suggest it is involved in the progression of GISTs (Haller et al., 2005; Perrone et al., 2005; Ricci et al., 2004; Sabah et al., 2004; Schneider-Stock et al., 2005). Consistent with previous data in current study the loss of 9p is most frequently seen in malignant tumors further supporting the involvement of *CDKN2A/2B* in the progression of GIST. The involvement of all three tumor suppressors (p16^{INK4a}, p14^{ARF} and p15^{INK4b}) in GIST tumorigenesis was recently investigated by Perrone et al. They found the loss of p16^{INK4a} mRNA in over 40% of malignant GISTs. Furthermore, loss of p16^{INK4a} was always coupled with p14^{ARF} loss (Perrone et al., 2005). The results of current study support these earlier findings and confirm the copy number loss of *CDKN2A/2B* genes in malignant GISTs as detected by array CGH. Additionally the pattern produced by the minimal common overlapping areas at 9p and the fact that in one sample the aberration forms a breakpoint of a loss and gain at 9p21.3 may indicate a possibility for a creation of fusion gene. However, further research is needed to address this issue. The high rate of 1p loss in both benign and malignant tumors found in current study does not correlate with some previous results relating 1p loss to malignancy (Gunawan et al., 2002; O'Leary et al., 1999). Nevertheless the result is consistent with the findings of El-Rifai et al. who found no statistical difference between GISTs of different grade concerning the loss of 1p. Further supporting this finding 22 samples used in the current study were also included in the study of El-Rifai et al. (El-Rifai et al., 2000a). The discrepancy in this issue maybe due to different approaches used in defining the grade of GISTs.

The results of current research identified a copy number loss of *ENO1* also know as *MYC* promoter-binding protein 1. This gene located at 1p36.23 codes for an enzyme with many functions e.g. in glycolysis and growth control. Importantly ENO1 binds to MYC; a transcription factor located at 8q24.12-q24.13 and found as a recurrent copy number gain in this study. The binding of ENO1 represses the expression of MYC and prevents the stimulation of cell proliferation (Feo et al., 2000). A concurrent copy number loss of *ENO1* and a gain of *MYC* could explain both the presence of 1p loss in benign tumors and the malignancy of 8q gain. An alternative suppression mechanism of *MYC* could be sufficient to keep cell proliferation in control in benign tumors representing 1p loss but an added 8q gain would increase gene dosage of *MYC* to such a level that without the suppression of *ENO1* the tumor cells would spread with malignant consequences. It has been demonstrated earlier that the expression of *c-MYC* has some prognostic value in the evaluation of malignancy of GISTs (Panizo-Santos et al., 2000). The findings of current study suggest that the copy number loss of *ENO1* at 1p36.23 and a copy number gain of *MYC* at 8q24.12-q24.13 are important cytogenetic changes involved in the progression of GIST and that these genes together have a central role in these events. Furthermore, the results suggest that there is a link between chromosomal aberrations in 1p and 8q and that the loss of *ENO1* occurs before the gain of *MYC*. However, further research including gene- and protein expression studies are needed to establish the function of *MYC* and *ENO1* in GIST tumorigenesis. In many tumors mutations in *NF2* lead to genetic inactivation and consequent loss of Merlin expression. Fukasawa et al. have suggested that *NF2* plays a role in GIST pathogenesis (Fukasawa et al., 2000). However, *NF2* mutations were later studied by Pylkkänen et al., and Lasota et al., with negative results, and according to Pylkkänen et al., Merlin is expressed in GISTs (Lasota et al., 2005; Pylkkanen et al., 2003). The *NF2* gene was found as copy number loss in 63% of all tumors in the current sample series indicating that it might be a target gene of 22q loss. However, the minimal common overlapping area of aberration excluded *NF2* locus and most samples representing a copy number loss of *NF2* had a loss of whole q arm. Thus the role of *NF2* and copy number losses in chromosome 22 remains to be investigated.

Despite the fact that the minimal common overlapping area identified in chromosome 4 is located outside the *KIT* locus a copy number gain at this locus on 4q12 was detected in

five samples. All samples featured a gain of whole q-arm but nevertheless had a copy number loss of *KIT* gene as seen from the aCGH data. The current results support the claim that KIT overexpression and *KIT* amplification are rarely related (Tabone et al., 2005). However, the gain of *KIT* might have some other consequences that play a role in the molecular pathogenesis of GIST. Unfortunately the mutational status of KIT and *PDGFRA* was only available from one of the samples displaying the gain of *KIT*. Consequently it was not possible to study the relationship between *KIT* mutations and copy number gain. Furthermore, none of the patients featuring *KIT* gain had been treated with imatinib and therefore we were unable to study the previous finding that *c-KIT* amplification may cause resistance to imatinib (Debiec-Rychter et al., 2005). Another candidate oncogene for GIST was identified at chromosome 12. *MDM2* was found as a copy number gain in three samples suggesting that it may act as an oncogene in a subset of GISTs. We suggest further molecular and cytogenetic studies in relation to 12q15 gain. A recent study investigated the involvement of nine known oncogenes in the genomic rearrangements of GIST. Two of the investigated oncogenes, *CMYC* and *MDM2* were also found as a copy number gain in the current study indicating them as possible target genes of these chromosomal aberrations (Tornillo et al., 2005). In conclusion, for the first time in the research of sporadic gastrointestinal sromal tumors the method of array CGH was applied in present study. As a result new target genes of chromosomal aberrations were identified. Genes represented as a copy number loss in present study are *SIVA, PARP2 , APEX1* and *NDRG2* in chromosome 14, *NF2* at chromosome 22, *CDKN2A/2B* at 9p and *ENO1* at 1p. Genes found as a copy number gain are *KIT* at 4q, *MYC* at 8q and *MDM2* at 12q. Array CGH proofed to be an effective method for the identification of candidate genes involved in the development and progression of GISTs. Further molecular- and cell biology studies on the identified genes are suggested.

6. References

Antonescu, C.R., Besmer, P., Guo, T., Arkun, K., Hom, G., Koryotowski, B., Leversha, M.A., Jeffrey, P.D., Desantis, D., Singer, S., Brennan, M.F., Maki, R.G., and DeMatteo, R.P. 2005. Acquired resistance to imatinib in gastrointestinal stromal tumor occurs through secondary gene mutation. *Clin.Cancer Res.* 11:4182-4190.

Atiye, J., Wolf, M., Kaur, S., Monni, O., Bohling, T., Kivioja, A., Tas, E., Serra, M., Tarkkanen, M., and Knuutila, S. 2005. Gene amplifications in osteosarcoma-CGH microarray analysis. *Genes Chromosomes Cancer.* 42:158-163.

Barrett, M.T., Scheffer, A., Ben-Dor, A., Sampas, N., Lipson, D., Kincaid, R., Tsang, P., Curry, B., Baird, K., Meltzer, P.S., Yakhini, Z., Bruhn, L., and Laderman, S. 2004. Comparative genomic hybridization using oligonucleotide microarrays and total genomic DNA. *Proc.Natl.Acad.Sci.U.S.A.* 101:17765-17770.

Baudis, M., and Cleary, M.L. 2001. Progenetix.net: an online repository for molecular cytogenetic aberration data. *Bioinformatics.* 17:1228-1229.

Bennicelli, J.L., and Barr, F.G. 1999. Genetics and the biologic basis of sarcomas. *Curr.Opin.Oncol.* 11:267-274.

Besmer, P., Murphy, J.E., George, P.C., Qiu, F.H., Bergold, P.J., Lederman, L., Snyder, H.W.,Jr, Brodeur, D., Zuckerman, E.E., and Hardy, W.D. 1986. A new acute transforming feline retrovirus and relationship of its oncogene v-kit with the protein kinase gene family. *Nature.* 320:415-421.

Blume-Jensen, P., Claesson-Welsh, L., Siegbahn, A., Zsebo, K.M., Westermark, B., and Heldin, C.H. 1991. Activation of the human c-kit product by ligand-induced dimerization mediates circular actin reorganization and chemotaxis. *EMBO J.* 10:4121-4128.

Breiner, J.A., Meis-Kindblom, J., Kindblom, L.G., McComb, E., Liu, J., Nelson, M., and Bridge, J.A. 2000. Loss of 14q and 22q in gastrointestinal stromal tumors (pacemaker cell tumors). *Cancer Genet.Cytogenet.* 120:111-116.

Buchdunger, E., Cioffi, C.L., Law, N., Stover, D., Ohno-Jones, S., Druker, B.J., and Lydon, N.B. 2000. Abl protein-tyrosine kinase inhibitor STI571 inhibits in vitro signal transduction mediated by c-kit and platelet-derived growth factor receptors. *J.Pharmacol.Exp.Ther.* 295:139-145.

Carvalho, B., Ouwerkerk, E., Meijer, G.A., and Ylstra, B. 2004. High resolution microarray comparative genomic hybridisation analysis using spotted oligonucleotides. *J.Clin.Pathol.* 57:644-646.

Chen, Y., Tzeng, C.C., Liou, C.P., Chang, M.Y., Li, C.F., and Lin, C.N. 2004. Biological significance of chromosomal imbalance aberrations in gastrointestinal stromal tumors. *J.Biomed.Sci.* 11:65-71.

Corless, C.L., Fletcher, J.A., and Heinrich, M.C. 2004. Biology of gastrointestinal stromal tumors. *J.Clin.Oncol.* 22:3813-3825.

Dai, Y.C., Ho, C.L., Tsai, Y.C., Hsu, Y.H., Chang, Y.C., Liu, H.S., Chen, H.H., and Chow, N.H. 2005. Allelic loss of 14q32 in the pathogenesis of gastrointestinal and ampullary malignancies: mapping of the target region to a 17 cM interval. *J.Cancer Res.Clin.Oncol.* 131:94-100.

Debiec-Rychter, M., Cools, J., Dumez, H., Sciot, R., Stul, M., Mentens, N., Vranckx, H., Wasag, B., Prenen, H., Roesel, J., Hagemeijer, A., Van Oosterom, A., and Marynen, P. 2005. Mechanisms of resistance to imatinib mesylate in gastrointestinal stromal tumors and activity of the PKC412 inhibitor against imatinib-resistant mutants. *Gastroenterology.* 128:270-279.

Debiec-Rychter, M., Lasota, J., Sarlomo-Rikala, M., Kordek, R., and Miettinen, M. 2001a. Chromosomal aberrations in malignant gastrointestinal stromal tumors: correlation with c-KIT gene mutation. *Cancer Genet.Cytogenet.* 128:24-30.

Debiec-Rychter, M., Sciot, R., Pauwels, P., Schoenmakers, E., Dal Cin, P., and Hagemeijer, A. 2001b. Molecular cytogenetic definition of three distinct chromosome arm 14q deletion intervals in gastrointestinal stromal tumors. *Genes Chromosomes Cancer.* 32:26-32.

Debiec-Rychter, M., Wasag, B., Stul, M., De Wever, I., Van Oosterom, A., Hagemeijer, A., and Sciot, R. 2004. Gastrointestinal stromal tumours (GISTs) negative for KIT (CD117 antigen) immunoreactivity. *J.Pathol.* 202:430-438.

Dematteo, R.P., Heinrich, M.C., El-Rifai, W.M., and Demetri, G. 2002. Clinical management of gastrointestinal stromal tumors: before and after STI-571. *Hum.Pathol.* 33:466-477.

Demetri, G.D., von Mehren, M., Blanke, C.D., Van den Abbeele, A.D., Eisenberg, B., Roberts, P.J., Heinrich, M.C., Tuveson, D.A., Singer, S., Janicek, M., Fletcher, J.A., Silverman, S.G., Silberman, S.L., Capdeville, R., Kiese, B., Peng, B., Dimitrijevic, S., Druker, B.J., Corless, C., Fletcher, C.D., and Joensuu, H. 2002. Efficacy and safety of imatinib mesylate in advanced gastrointestinal stromal tumors. *N.Engl.J.Med.* 347:472-480.

Deng, Y., Yao, L., Chau, L., Ng, S.S., Peng, Y., Liu, X., Au, W.S., Wang, J., Li, F., Ji, S., Han, H., Nie, X., Li, Q., Kung, H.F., Leung, S.Y., and Lin, M.C. 2003. N-Myc downstream-regulated gene 2 (NDRG2) inhibits glioblastoma cell proliferation. *Int.J.Cancer.* 106:342-347.

Druker, B.J., Tamura, S., Buchdunger, E., Ohno, S., Segal, G.M., Fanning, S., Zimmermann, J., and Lydon, N.B. 1996. Effects of a selective inhibitor of the Abl tyrosine kinase on the growth of Bcr-Abl positive cells. *Nat.Med.* 2:561-566.

El-Rifai, W., Sarlomo-Rikala, M., Andersson, L.C., Knuutila, S., and Miettinen, M. 2000a. DNA sequence copy number changes in gastrointestinal stromal tumors: tumor progression and prognostic significance. *Cancer Res.* 60:3899-3903.

El-Rifai, W., Sarlomo-Rikala, M., Andersson, L.C., Miettinen, M., and Knuutila, S. 2000b. High-resolution deletion mapping of chromosome 14 in stromal tumors of the gastrointestinal tract suggests two distinct tumor suppressor loci. *Genes Chromosomes Cancer.* 27:387-391.

el-Rifai, W., Sarlomo-Rikala, M., Miettinen, M., Knuutila, S., and Andersson, L.C. 1996. DNA copy number losses in chromosome 14: an early change in gastrointestinal stromal tumors. *Cancer Res.* 56:3230-3233.

Enders, G.H. 2003. The INK4a/ARF locus and human cancer. *Methods Mol.Biol.* 222:197-209.

Fearon, E.R. 1997. Human cancer syndromes: clues to the origin and nature of cancer. *Science.* 278:1043-1050.

Feo, S., Arcuri, D., Piddini, E., Passantino, R., and Giallongo, A. 2000. ENO1 gene product binds to the c-myc promoter and acts as a transcriptional repressor: relationship with Myc promoter-binding protein 1 (MBP-1). *FEBS Lett.* 473:47-52.

Fletcher, C.D., Berman, J.J., Corless, C., Gorstein, F., Lasota, J., Longley, B.J., Miettinen, M., O'Leary, T.J., Remotti, H., Rubin, B.P., Shmookler, B., Sobin, L.H., and Weiss, S.W. 2002. Diagnosis of gastrointestinal stromal tumors: a consensus approach. *Int.J.Surg.Pathol.* 10:81-89.

Fukasawa, T., Chong, J.M., Sakurai, S., Koshiishi, N., Ikeno, R., Tanaka, A., Matsumoto, Y., Hayashi, Y., Koike, M., and Fukayama, M. 2000. Allelic loss of 14q and 22q, NF2 mutation, and genetic instability occur independently of c-kit mutation in gastrointestinal stromal tumor. *Jpn.J.Cancer Res.* 91:1241-1249.

Gervasio Martin-Lorenzo, J., Aguayo-Albasini, J.L., Torralba-Martinez, J.A., Liron-Ruiz, R., Gimenez-Bascunana, A., Miquel-Perello, J., Moreno-Egea, A., and Carrasco-Gonzalez, L. 2006. Gastrointestinal stromal tumors. Diagnosis, prognosis and current surgical treatment.Follow-up of 18 treated patients. *Cir.Esp.* 79:22-27.

Ghazani, A.A., Arneson, N.C., Warren, K., and Done, S.J. 2006. Limited tissue fixation times and whole genomic amplification do not impact array CGH profiles. *J.Clin.Pathol.* 59:311-315.

Goettsch, W.G., Bos, S.D., Breekveldt-Postma, N., Casparie, M., Herings, R.M., and Hogendoorn, P.C. 2005. Incidence of gastrointestinal stromal tumours is underestimated: results of a nation-wide study. *Eur.J.Cancer.* 41:2868-2872.

Gunawan, B., Bergmann, F., Hoer, J., Langer, C., Schumpelick, V., Becker, H., and Fuzesi, L. 2002. Biological and clinical significance of cytogenetic abnormalities in low-risk and high-risk gastrointestinal stromal tumors. *Hum.Pathol.* 33:316-321.

Haller, F., Gunawan, B., von Heydebreck, A., Schwager, S., Schulten, H.J., Wolf-Salgo, J., Langer, C., Ramadori, G., Sultmann, H., and Fuzesi, L. 2005. Prognostic role of E2F1 and members of the CDKN2A network in gastrointestinal stromal tumors. *Clin.Cancer Res.* 11:6589-6597.

Hannon, G.J., and Beach, D. 1994. p15INK4B is a potential effector of TGF-beta-induced cell cycle arrest. *Nature.* 371:257-261.

Heinrich, M.C., Corless, C.L., Demetri, G.D., Blanke, C.D., von Mehren, M., Joensuu, H., McGreevey, L.S., Chen, C.J., Van den Abbeele, A.D., Druker, B.J., Kiese, B., Eisenberg, B., Roberts, P.J., Singer, S., Fletcher, C.D., Silberman, S., Dimitrijevic, S., and Fletcher, J.A. 2003a. Kinase mutations and imatinib response in patients with metastatic gastrointestinal stromal tumor. *J.Clin.Oncol.* 21:4342-4349.

Heinrich, M.C., Corless, C.L., Duensing, A., McGreevey, L., Chen, C.J., Joseph, N., Singer, S., Griffith, D.J., Haley, A., Town, A., Demetri, G.D., Fletcher, C.D., and Fletcher, J.A. 2003b. PDGFRA activating mutations in gastrointestinal stromal tumors. *Science.* 299:708-710.

Heinrich, M.C., Rubin, B.P., Longley, B.J., and Fletcher, J.A. 2002. Biology and genetic aspects of gastrointestinal stromal tumors: KIT activation and cytogenetic alterations. *Hum.Pathol.* 33:484-495.

Hirota, S., and Isozaki, K. 2006. Pathology of gastrointestinal stromal tumors. *Pathol.Int.* 56:1-9.

Hirota, S., Isozaki, K., Moriyama, Y., Hashimoto, K., Nishida, T., Ishiguro, S., Kawano, K., Hanada, M., Kurata, A., Takeda, M., Muhammad Tunio, G., Matsuzawa, Y., Kanakura, Y., Shinomura, Y., and Kitamura, Y. 1998. Gain-of-function mutations of c-kit in human gastrointestinal stromal tumors. *Science.* 279:577-580.

Hirota, S., Ohashi, A., Nishida, T., Isozaki, K., Kinoshita, K., Shinomura, Y., and Kitamura, Y. 2003. Gain-of-function mutations of platelet-derived growth factor receptor alpha gene in gastrointestinal stromal tumors. *Gastroenterology.* 125:660-667.

Referred to March 22, 2006
http://en.wikipedia.org/wiki/Karyotype

Referred to June 4, 2005
http://genome.ucsc.edu/

Referred to March 22, 2006
http://members.aol.com/chrominfo/fishinfo.htm

Referred to March 22, 2006
http://wsrv.clas.virginia.edu/~rjh9u/ideo.html

Referred to December 15, 2005
http://www.ensembl.org/index.html

Referrred to June 4, 2005
http://www.few.vu.nl/~vumarray/

Referred to December 20, 2005
http://www.genecards.org/

Referred to March 31, 2006
http://www.lucia-cytogenetics.com/index.php?inc=cgh&lang=en

Referred to March 23, 2006
http://www.pathology.washington.edu/research/cytopages/

Referred to December 13, 2005
 http://www.progenetix.net

Hu, X.L., Liu, X.P., Lin, S.X., Deng, Y.C., Liu, N., Li, X., and Yao, L.B. 2004. NDRG2 expression and mutation in human liver and pancreatic cancers. *World J.Gastroenterol.* 10:3518-3521.

Isozaki, K., Terris, B., Belghiti, J., Schiffmann, S., Hirota, S., and Vanderwinden, J.M. 2000. Germline-activating mutation in the kinase domain of KIT gene in familial gastrointestinal stromal tumors. *Am.J.Pathol.* 157:1581-1585.

Joensuu, H., Roberts, P.J., Sarlomo-Rikala, M., Andersson, L.C., Tervahartiala, P., Tuveson, D., Silberman, S., Capdeville, R., Dimitrijevic, S., Druker, B., and Demetri, G.D. 2001. Effect of the tyrosine kinase inhibitor STI571 in a patient with a metastatic gastrointestinal stromal tumor. *N.Engl.J.Med.* 344:1052-1056.

Johansson, M. 1999. A human poly(ADP-ribose) polymerase gene family (ADPRTL): cDNA cloning of two novel poly(ADP-ribose) polymerase homologues. *Genomics.* 57:442-445.

Jong, K., Marchiori, E., Meijer, G., Vaart, A.V., and Ylstra, B. 2004. Breakpoint identification and smoothing of array comparative genomic hybridization data. *Bioinformatics.* 20:3636-3637.

Kallioniemi, A., Kallioniemi, O.P., Sudar, D., Rutovitz, D., Gray, J.W., Waldman, F., and Pinkel, D. 1992. Comparative genomic hybridization for molecular cytogenetic analysis of solid tumors. *Science.* 258:818-821.

Kamb, A., Gruis, N.A., Weaver-Feldhaus, J., Liu, Q., Harshman, K., Tavtigian, S.V., Stockert, E., Day, R.S.,3rd, Johnson, B.E., and Skolnick, M.H. 1994. A cell cycle regulator potentially involved in genesis of many tumor types. *Science.* 264:436-440.

Kim, N.G., Kim, J.J., Ahn, J.Y., Seong, C.M., Noh, S.H., Kim, C.B., Min, J.S., and Kim, H. 2000. Putative chromosomal deletions on 9P, 9Q and 22Q occur preferentially in malignant gastrointestinal stromal tumors. *Int.J.Cancer.* 85:633-638.

Kindblom, L.G., Remotti, H.E., Aldenborg, F., and Meis-Kindblom, J.M. 1998. Gastrointestinal pacemaker cell tumor (GIPACT): gastrointestinal stromal tumors show phenotypic characteristics of the interstitial cells of Cajal. *Am.J.Pathol.* 152:1259-1269.

Knuutila, S., Armengol, G., Bjorkqvist, A.M., el-Rifai, W., Larramendy, M.L., Monni, O., and Szymanska, J. 1998. Comparative genomic hybridization study on pooled DNAs from tumors of one clinical-pathological entity. *Cancer Genet.Cytogenet.* 100:25-30.

Ko, J.M., Yau, W.L., Chan, P.L., Lung, H.L., Yang, L., Lo, P.H., Tang, J.C., Srivastava, G., Stanbridge, E.J., and Lung, M.L. 2005. Functional evidence of decreased tumorigenicity associated with monochromosome transfer of chromosome 14 in esophageal cancer and the mapping of tumor-suppressive regions to 14q32. *Genes Chromosomes Cancer.* 43:284-293.

Lasota, J., Wozniak, A., Kopczynski, J., Dansonka-Mieszkowska, A., Wasag, B., Mitsuhashi, T., Sarlomo-Rikala, M., Lee, J.R., Schneider-Stock, R., Stachura, J., Limon, J., and Miettinen, M. 2005. Loss of heterozygosity on chromosome 22q in gastrointestinal stromal tumors (GISTs): a study on 50 cases. *Lab.Invest.* 85:237-247.

Ludolph, T., Schweitzer, A., Bremer, A., Schulz, U., and Glasbrenner, B. 2006. Gastrointestinal Stromal Tumors (GIST). Clinical Characteristics, Diagnosis, and Therapy in Five Cases. *Med.Klin.(Munich).* 101:69-74.

Lusis, E.A., Watson, M.A., Chicoine, M.R., Lyman, M., Roerig, P., Reifenberger, G., Gutmann, D.H., and Perry, A. 2005. Integrative genomic analysis identifies NDRG2 as a candidate tumor suppressor gene frequently inactivated in clinically aggressive meningioma. *Cancer Res.* 65:7121-7126.

Ma, Y., Zeng, S., Metcalfe, D.D., Akin, C., Dimitrijevic, S., Butterfield, J.H., McMahon, G., and Longley, B.J. 2002. The c-KIT mutation causing human mastocytosis is resistant to STI571 and other KIT kinase inhibitors; kinases with enzymatic site mutations show different inhibitor sensitivity profiles than wild-type kinases and those with regulatory-type mutations. *Blood.* 99:1741-1744.

Majumder, S., Brown, K., Qiu, F.H., and Besmer, P. 1988. c-kit protein, a transmembrane kinase: identification in tissues and characterization. *Mol.Cell.Biol.* 8:4896-4903.

Mantripragada, K.K., Buckley, P.G., de Stahl, T.D., and Dumanski, J.P. 2004. Genomic microarrays in the spotlight. *Trends Genet.* 20:87-94.

Medeiros, F., Corless, C.L., Duensing, A., Hornick, J.L., Oliveira, A.M., Heinrich, M.C., Fletcher, J.A., and Fletcher, C.D. 2004. KIT-negative gastrointestinal stromal tumors: proof of concept and therapeutic implications. *Am.J.Surg.Pathol.* 28:889-894.

Miettinen, M., El-Rifai, W., H L Sobin, L., and Lasota, J. 2002. Evaluation of malignancy and prognosis of gastrointestinal stromal tumors: a review. *Hum.Pathol.* 33:478-483.

Miller, S.A., Dykes, D.D., and Polesky, H.F. 1988. A simple salting out procedure for extracting DNA from human nucleated cells. *Nucleic Acids Res.* 16:1215.

Mol, C.D., Dougan, D.R., Schneider, T.R., Skene, R.J., Kraus, M.L., Scheibe, D.N., Snell, G.P., Zou, H., Sang, B.C., and Wilson, K.P. 2004. Structural basis for the autoinhibition and STI-571 inhibition of c-Kit tyrosine kinase. *J.Biol.Chem.* 279:31655-31663.

Mudan, S.S., Conlon, K.C., Woodruff, J.M., Lewis, J.J., and Brennan, M.F. 2000. Salvage surgery for patients with recurrent gastrointestinal sarcoma: prognostic factors to guide patient selection. *Cancer.* 88:66-74.

Nakahara, M., Isozaki, K., Hirota, S., Miyagawa, J., Hase-Sawada, N., Taniguchi, M., Nishida, T., Kanayama, S., Kitamura, Y., Shinomura, Y., and Matsuzawa, Y. 1998. A novel gain-of-function mutation of c-kit gene in gastrointestinal stromal tumors. *Gastroenterology.* 115:1090-1095.

Nishida, T., Hirota, S., Taniguchi, M., Hashimoto, K., Isozaki, K., Nakamura, H., Kanakura, Y., Tanaka, T., Takabayashi, A., Matsuda, H., and Kitamura, Y. 1998. Familial gastrointestinal stromal tumours with germline mutation of the KIT gene. *Nat.Genet.* 19:323-324.

Okuda, T., and Kondoh, H. 1999. Identification of new genes ndr2 and ndr3 which are related to Ndr1/RTP/Drg1 but show distinct tissue specificity and response to N-myc. *Biochem.Biophys.Res.Commun.* 266:208-215.

O'Leary, T., Ernst, S., Przygodzki, R., Emory, T., and Sobin, L. 1999. Loss of heterozygosity at 1p36 predicts poor prognosis in gastrointestinal stromal/smooth muscle tumors. *Lab.Invest.* 79:1461-1467.

Panizo-Santos, A., Sola, I., Vega, F., de Alava, E., Lozano, M.D., Idoate, M.A., and Pardo-Mindan, J. 2000. Predicting Metastatic Risk of Gastrointestinal Stromal Tumors: Role of Cell Proliferation and Cell Cycle Regulatory Proteins. *Int.J.Surg.Pathol.* 8:133-144.

Perrone, F., Tamborini, E., Dagrada, G.P., Colombo, F., Bonadiman, L., Albertini, V., Lagonigro, M.S., Gabanti, E., Caramuta, S., Greco, A., Torre, G.D., Gronchi, A., Pierotti, M.A., and Pilotti, S. 2005. 9p21 locus analysis in high-risk gastrointestinal stromal tumors characterized for c-kit and platelet-derived growth factor receptor alpha gene alterations. *Cancer.* 104:159-169.

Pinkel, D., and Albertson, D.G. 2005. Comparative genomic hybridization. *Annu.Rev.Genomics Hum.Genet.* 6:331-354.

Pinkel, D., Segraves, R., Sudar, D., Clark, S., Poole, I., Kowbel, D., Collins, C., Kuo, W.L., Chen, C., Zhai, Y., Dairkee, S.H., Ljung, B.M., Gray, J.W., and Albertson, D.G. 1998. High resolution analysis of DNA copy number variation using comparative genomic hybridization to microarrays. *Nat.Genet.* 20:207-211.

Pollack, J.R., Perou, C.M., Alizadeh, A.A., Eisen, M.B., Pergamenschikov, A., Williams, C.F., Jeffrey, S.S., Botstein, D., and Brown, P.O. 1999. Genome-wide analysis of DNA copy-number changes using cDNA microarrays. *Nat.Genet.* 23:41-46.

Prasad, K.V., Ao, Z., Yoon, Y., Wu, M.X., Rizk, M., Jacquot, S., and Schlossman, S.F. 1997. CD27, a member of the tumor necrosis factor receptor family, induces apoptosis and binds to Siva, a proapoptotic protein. *Proc.Natl.Acad.Sci.U.S.A.* 94:6346-6351.

Pylkkanen, L., Sarlomo-Rikala, M., Wessman, M., Hamalainen, E., Sainio, M., Husgafvel-Pursiainen, K., and Carpen, O. 2003. Chromosome 22q alterations and expression of the NF2 gene product, merlin, in gastrointestinal stromal tumors. *Hum.Pathol.* 34:872-879.

Quackenbush, J. 2002. Microarray data normalization and transformation. *Nat.Genet.* 32 Suppl:496-501.

Ricci, R., Arena, V., Castri, F., Martini, M., Maggiano, N., Murazio, M., Pacelli, F., Potenza, A.E., Vecchio, F.M., and Larocca, L.M. 2004. Role of p16/INK4a in gastrointestinal stromal tumor progression. *Am.J.Clin.Pathol.* 122:35-43.

Robson, C.N., and Hickson, I.D. 1991. Isolation of cDNA clones encoding a human apurinic/apyrimidinic endonuclease that corrects DNA repair and mutagenesis defects in E. coli xth (exonuclease III) mutants. *Nucleic Acids Res.* 19:5519-5523.

Rossi, G., Valli, R., Bertolini, F., Marchioni, A., Cavazza, A., Mucciarini, C., Migaldi, M., Federico, M., Trentini, G.P., and Sgambato, A. 2005. PDGFR expression in differential diagnosis between KIT-negative gastrointestinal stromal tumours and other primary soft-tissue tumours of the gastrointestinal tract. *Histopathology.* 46:522-531.

Rubin, B.P., Singer, S., Tsao, C., Duensing, A., Lux, M.L., Ruiz, R., Hibbard, M.K., Chen, C.J., Xiao, S., Tuveson, D.A., Demetri, G.D., Fletcher, C.D., and Fletcher, J.A. 2001. KIT activation is a ubiquitous feature of gastrointestinal stromal tumors. *Cancer Res.* 61:8118-8121.

Sabah, M., Cummins, R., Leader, M., and Kay, E. 2004. Loss of heterozygosity of chromosome 9p and loss of p16INK4A expression are associated with malignant gastrointestinal stromal tumors. *Mod.Pathol.* 17:1364-1371.

Sanchez, B.R., Morton, J.M., Curet, M.J., Alami, R.S., and Safadi, B.Y. 2005. Incidental finding of gastrointestinal stromal tumors (GISTs) during laparoscopic gastric bypass. *Obes.Surg.* 15:1384-1388.

Sarlomo-Rikala, M., El-Rifai, W., Lahtinen, T., Andersson, L.C., Miettinen, M., and Knuutila, S. 1998a. Different patterns of DNA copy number changes in gastrointestinal stromal tumors, leiomyomas, and schwannomas. *Hum.Pathol.* 29:476-481.

Sarlomo-Rikala, M., Kovatich, A.J., Barusevicius, A., and Miettinen, M. 1998b. CD117: a sensitive marker for gastrointestinal stromal tumors that is more specific than CD34. *Mod.Pathol.* 11:728-734.

Schneider-Stock, R., Boltze, C., Lasota, J., Peters, B., Corless, C.L., Ruemmele, P., Terracciano, L., Pross, M., Insabato, L., Di Vizio, D., Iesalnieks, I., Dirnhofer, S., Hartmann, A., Heinrich, M., Miettinen, M., Roessner, A., and Tornillo, L. 2005. Loss of p16 protein defines high-risk patients with gastrointestinal stromal tumors: a tissue microarray study. *Clin.Cancer Res.* 11:638-645.

Serrano, M., Hannon, G.J., and Beach, D. 1993. A new regulatory motif in cell-cycle control causing specific inhibition of cyclin D/CDK4. *Nature.* 366:704-707.

Solinas-Toldo, S., Lampel, S., Stilgenbauer, S., Nickolenko, J., Benner, A., Dohner, H., Cremer, T., and Lichter, P. 1997. Matrix-based comparative genomic hybridization: biochips to screen for genomic imbalances. *Genes Chromosomes Cancer.* 20:399-407.

Tabone, S., Theou, N., Wozniak, A., Saffroy, R., Deville, L., Julie, C., Callard, P., Lavergne-Slove, A., Debiec-Rychter, M., Lemoine, A., and Emile, J.F. 2005. KIT overexpression and amplification in gastrointestinal stromal tumors (GISTs). *Biochim.Biophys.Acta.* 1741:165-172.

Thomas D. Gelehrter, Francis S., Principles of medical genetics, Baltimore: Williams & Wilkins, 2nd edition 1998

Tornillo, L., Duchini, G., Carafa, V., Lugli, A., Dirnhofer, S., Di Vizio, D., Boscaino, A., Russo, R., Tapia, C., Schneider-Stock, R., Sauter, G., Insabato, L., and Terracciano, L.M. 2005. Patterns of gene amplification in gastrointestinal stromal tumors (GIST). *Lab.Invest.* 85:921-931.

Tuveson, D.A., Willis, N.A., Jacks, T., Griffin, J.D., Singer, S., Fletcher, C.D., Fletcher, J.A., and Demetri, G.D. 2001. STI571 inactivation of the gastrointestinal stromal tumor c-KIT oncoprotein: biological and clinical implications. *Oncogene.* 20:5054-5058.

Wakai, T., Kanda, T., Hirota, S., Ohashi, A., Shirai, Y., and Hatakeyama, K. 2004. Late resistance to imatinib therapy in a metastatic gastrointestinal stromal tumour is associated with a second KIT mutation. *Br.J.Cancer.* 90:2059-2061.

Wang, G., Brennan, C., Rook, M., Wolfe, J.L., Leo, C., Chin, L., Pan, H., Liu, W.H., Price, B., and Makrigiorgos, G.M. 2004. Balanced-PCR amplification allows unbiased identification of genomic copy changes in minute cell and tissue samples. *Nucleic Acids Res.* 32:e76.

Yi, E.S., Strong, C.R., Piao, Z., Perucho, M., and Weidner, N. 2005. Epithelioid gastrointestinal stromal tumor with PDGFRA activating mutation and immunoreactivity. *Appl.Immunohistochem.Mol.Morphol.* 13:157-161.

Zalcberg, J.R., Verweij, J., Casali, P.G., Le Cesne, A., Reichardt, P., Blay, J.Y., Schlemmer, M., Van Glabbeke, M., Brown, M., Judson, I.R., EORTC Soft Tissue and Bone Sarcoma Group, the Italian Sarcoma Group., and Australasian Gastrointestinal Trials Group. 2005. Outcome of patients with advanced gastro-intestinal stromal tumours crossing over to a daily imatinib dose of 800 mg after progression on 400 mg. *Eur.J.Cancer.* 41:1751-1757.

Appendices

Appendix 1 Preparation of Solutions

The following solutions were provided by HUSLAB Media Production Unit.

Lysis Buffer

1M Tris-HCl pH 8.5	15 ml
0.5M EDTA	600 µl
Tween-20	1.5 ml
dH$_2$O	add to 300 ml

RNAase

Dissolve 100mg haiman RNAase (Roche Cat. No. 109169) into 25 ml dH$_2$O
Incubate at 100°C heat block for 15 minutes. Divide into aliquots of 1 ml and store at -20°C.

Buffer B

3M NaCl	25 ml
0,1M EDTA pH 8	250 ml
dH$_2$O	add to 1000 ml

Proteinase K

Dissolve 100mg of Proteinase K (Merck, Darmstadt, Germany, No. 1.24568.0500) into 100 ml of buffer B. Let dissolve for approximately 2h at +37°C.

TE-buffer Ph8

1M Tris Ph 8	50 ml
0.5M EDTA Ph 8	10 ml
dH$_2$O	add to 5000 ml

TKM1-buffer

1M Tris-HCl Ph 7.6	10 ml
2M Kcl	5 ml
1M $MgCl_2$	10 ml
0.5M EDTA Ph 7.6	4 ml
dH_2O	add to 1000 ml

TKM1 + Nonidet

Dissolve 25 ml of nonionic detergent Igepal CA-630 (Sigma-Aldricht Cat. No. I-3021) into 975 ml of TKM1-buffer.

TKM2-buffer

1M Tris-HCl Ph 7.6	10 ml
2M Kcl	5 ml
1M $MgCl_2$	10 ml
0.5M EDTA Ph 7.6	4 ml
5M NaCl	80 ml
dH_2O	add to 1000 ml

Appendix 2 Hybridization Solutions cDNA microarray

10x dNTP mix (low T mix)

dATP   12 µl
dGTP   12 µl
dCTP   12 µl
dTTP   6 µl
TE-buffer pH 8   958 µl
UltraPure dNTP set Amersham Pharmacia Biotech Inc. Cat No. 27-2035-02

Yeast tRNA

Dissolve lyophilized yeast tRNA (Sigma-Aldrich Cat. No. R8759) into 5 ml of TE-buffer pH 8. Divide into aliquots and store at -20°C.

3xSSC

20xSSC   7,5 ml
dH$_2$O   42,5 ml

Blocking Solution (5xSSC/0,1% SDS)

20xSSC   250 ml
10% SDS   10 ml
dH$_2$O   740 ml
1% BSA fraction V (Roche Diagnostics Cat. No. 109 517) was dissolved to a 100 ml of blocking solution and used the same day.

Array Pre-treatment Washing Solutions

2xSSC
20xSSC   100 ml
dH_2O 900 ml

0,2xSSC
20xSSC   10 ml
dH_2O 990 ml

Post-hybridization Washes

0,5xSSC/0,1% SDS

20xSCS   25 ml
10% SDS   10 ml
dH_2O 965 ml

0,5xSSC/0,01% SDS

20xSCS   25 ml
10% SDS   1 ml
dH_2O 974 ml

0,06XSSC

20xSSC   3 ml
dH_2O 997ml

Appendix 3 Complete Results of Study

No.	PAD	PAD	sex/age	mutation	aCGH results cDNAarray	aCGH results oligoarray
1	GIST	benign	m/45	c-kit wt, PDGFRA exon 12	-1p36.22-p36.33, +1q25.3-q44, -3p25.2-p26.3, +3p24.1-p25.2, -3p11.1-p24.1, +3q26.1-q29, -3q11.1-q11.2, -8p12-p23.3, +8p11.21-p12,+8q21.12-q24.3, -14q, +17q23.2-q25.1,+18q23, -21, -19q13.12-q13.2, -19q13.2, -21	ne
2	GIST	benign	f/61	c-kit wt, PDGFRA exon 12	-1p, -3q, -12q24.22, -14q, -X	ne
3	GIST	benign	m/50	c-kit wt, PDGFRA exon 18	-1p, -1q21.1, -6p25.2-p25.3, +8q, -14q, -19q13.43, -Xp11.23-p11.3	ne
4	GIST	benign	f/65	c-kit exon 11, PDGFRA ne	-1p31.3-p36.33, -1q21.1-q23.3, -1q32.1-q44, -4p14-p16.3, -6p12.3-p21.33, -8q24.21-q24.3, -9q33.3-q34.3, -11p15.4-p15.5, 11p11.2-q13.5, -14q, -15q23-q25.1, -16, -17, -19, -20q13.2-q13.33, -21q22.3, -22q, -X	ne
5	GIST	benign	m/85	c-kit exon 11, PDGFRA ne	-14q, -22q	ne
6	GIST	benign	m/69	c-kit wt, PDGFRA wt	-1p, -11p11.2-p15.5, -14q11.2-q13.1, -14q23.33, -15q21.1-q26.1, -19q13.43, -22q, +Xp22.2-p22.33	-1p, -4q34.1, -11p, -13q12.11-q13.3, -14q11.2, -14q12, -15q14-q26.3, -22q
7	GIST	benign	f/67	c-kit exon 11, PDGFRA ne	-1p35.1-p35.3, -14q	ne

8	GIST	benign	m/53	c-kit exon 11, PDGFRA ne	-1p32.2-p36.33, -1q44, -3p21.1-p21.31, -4p16.1-p16.3, -6p12.3-p22.1, -8q24.3, -9q33.3-q34.3, -10q26.3, -11p15.4-p15.5, -11p11.2-q13.2, -12p13.31, -12q13.1-q13.2, -14q11.2, -14q23.3-q32.33, -16p11.2-p13.3, -16q12.1-q24.3,+16p11.2-q12, -17p13.3-q23.2, -17q23.2-q25.3, +17q23.2, -19p13.11-p13.3, -19q12-q13.43, +19p13.11-q12, -21q22.3, -22q11.1-q13.1, -22q13.1-q13.33	ne
9	GIST	benign	m/41	c-kit exon 11, PDGFRA ne	-1p31.3-p35.3, -4p15.32-p16.3, -6q14.1-q27, -8q24.22-q24.3, -9q33.3-q34.3, -11q13.2-q13.4, -12q24.32-q24.33, -16p13.3, -19, -22q	ne
10	GIST	benign	f/60	ne	-1p36.13-p36.33, +3p21.32-p26.3, +3p21.31-q29, +4p16.1-q35.1, +5, +6p21.3-p25.3, +6p21.1-q25.3, -7p21.3-p22.3, -8q24.3, -9q33.3-q34.3, -11p15.5, -11p11.2-q13.2, -14q32.13-q32.33, +17q21.31-q25.1, +18, -19, -21q22.2-q22.3, -22q, -Xp22.33	ne
11	GIST	benign	f/70	ne	-5q13.2, -14q23.2-q32.33, -Xp22.33, -Xq28	-5q13.1-q13.2, -14q, -Xp22.32, Xp21.1
12	GIST	benign	f/60	ne	-1p36.11-p36.33, -1q21.2-q23.2, -1q44, -3p21.31, -4p15.2-p16.3, +5p15.2-q13.3, -6p21.1-p21.3, -8q24.3, -9q33.2-q34.3, -11p15.4-p15.5, -11p11.2-q13.4, -12p13.31-p13.33, -12q13.13, -12q13.13-q14.2, -14q11.2-q21.1, -14q22.2-q32.33, -16, -17p13.1-p13.3, -17q24.1-q25.3, -19, -21q22.11-q22.3, -22q, -Xp22.32-p22.33	ne
13	GIST	benign	m/67	ne	-1p, -3p21.31, -11p11.2-p15.5, -14q, -19p13.11, -19q13.2	ne

14	GIST	benign	f/72	c-kit exon 11, PDGFRA wt	-1p32.1-p36.33, -3p14.3-p21.31, -4p15.33-p16.3, +4p16.1-q35.2, -6p21.31-p21.33, +6p21.3-p25.3, +7q11.23-q21.3, -7q21.3-q22.1, +8q12.1-q24.13, -8q24.13-q24.3, -9q33.1-q34.3, -11p15.4-p15.5, -11p11.2-q13.5, +12q15-q23.3, +13q, -14q, -16, -17, +18, -19, -20q13.3-q13.33, -21q22.3, +21q22.3, -22q	ne
15	GIST	benign	m	c-kit exon 11, PDGFRA wt	-1p, +1q21.1-q21.2, -4p16.3-q24, +1q23.3-q44, -6p21.1-p21.33, +7q22.1-q34, -7q22.1, +8q11.23-q24.3, -8p23.3-q11.21, -9p13.2-p24.3, -9q33.3-q34.3, + -11p15.4-p15.5, -11q12.1-q13.2, 12p12.3-q13.11, +12q14.1-q23.3, -12p12.3-p13.33, -14q11.2-q21.1, -14q23.1-q32.33, -15q, -16p13.3, -17q25.1-q25.3, -18p11.32, -20q13.33, -21, -22q, -X	
16	GIST	malignant	m/52	c-kit wt, PDGFRA wt	-1p36.22-p36.33, +1q31.2-q44, -3p25.2-p26.3, +3p25.2-q24.1, -3p13-p24.1, +3q26.1-3q29, -8p12-p23.3, +8p12-q11.21, -14q, -20q13.33, -21	ne
17	GIST	malignant	m/60	c-kit exon 11, PDGFRA ne	-1p, -1q11-q12, +3q25.2-q29, +3q11.2-q25.2, -5p15.2-p15.33, +8, +9p21.1-p24.3, -13, -14q11.2-q21.1, -15q, +16p12.3-p13.3, -21, -22q	-1p, +3q11.2-q25.32, +3q26.32-q29, -13, -14q11.2-q23.3, -15q, +16p13.11-p13.13, +16p13.3, -21q, -22q

18	GIST	malignant	f/88	c-kit exon 11, PDGFRA ne	-1p36.33-q23.2, -4p15.2-p16.3, -5p15.2-p15.33, -6p21.1-p21.3, -7q35-q36.3, -8p, -8q24.1-q24.3, -9p21.3-p24.1, -9p21.2-q34.3, +9p21.2, -10p15.3-q23.31, -11p15.4-p15.5, -11q12.2-q13.4, -12p13.33-q14.2, -14q11.2-q12, -14q23.3-q32.33, -16, -17p13.3-q21.32, -19, -21q22.3, -22q, -X	+1p36.13-p36.23, -1p35.3-p36.11, +1p34.3-p35.1, -1p12-p34.31, -3p13-p14.1, +3q26.32-q26.33, +5p15.33, +5p12-p15.1, +6p22.1-p22.2, +6q24.2, +7q31.32, -8p11.23-p23.3, +8q23.3, -8q24.13-q24.3, -9p13.2, +9p13.2-p21.1, -9p21.1, +9p21.2-p21.3, -9p21.3, +9p21.3-p22.2, -9p22.3-p23, +9p23, -9p23-p24.1 ,+9p24.3, -9q,-10p11.21-p15.2, +10p15.2-p15.3, -10q11.21-q23.2, +15q26.1, -17p13.1-p13.2, +17q21.31-q25.3, -22q, -X
19	GIST	malignant	m/44	c-kit exon 11, PDGFRA ne	+5, +7, -22q, +Xp22.33	-4q25, +4q28.3, +5, +7, +8q23.1, +12q241.2, +15q26.1, +17q21.31, -21q22.2, -22q
20	GIST	malignant	f/71	ne	-1p, -4p16.3-q21.1, -10, -14q32.32-q32.33, -15q, -22q	-1p, -4, -9p21.3, -10, -15, -22q
21	GIST	malignant	f/73	ne	-1p, -2p11.2, -2q, +5p15.33-q13.2, -9p24.3-q12, -11p15.5, -13, -14q, -15q, -18q11.2-q23, -19p13.3, -22q, -Xp22.32-p22.33	ne
22	GIST	malignant	f/46	ne	+2, +4q23-q35.2, -7q34-q36.3, -10q26.2-q26.3, -11q25, -14q, -15q, -17p13.3, +17q11.2-q25.3, -19q13.2-q13.43, -22q, +Xp11.3-p22.2	ne
23	GIST	malignant	f/46	c-kit exon 11, PDGFRA ne	+1p36.31-p36.33, +2q, +4q24-q35.1, -7p13-p15.3, -7q33-q36.3, +8q22.3-q24.3, +9q34.3, -14q, +16p13.3, +17q11.2-q25.3, -19q13-q13.43, +20q13.33, -22q12.3-q13.31	ne
24	GIST	malignant	f/46	ne	-1p36.11-p36.33, +2p24-q37.3, +3q29, +4q11-q35.2, -7p13-p15.3, -7p22.3, -7q34-q36.3, +8q22.2-q24.22, -11, -14q23.1-q32.33, 15q14-q26.3, +16q11.2-q12.1, +17q11.2-q25.3, -19p13.3, -19q13.2-q13.43, -22q13.1-q13.33, -Xp22.32-p22.33	+2p23.3, +2p25.3, +2q, +4q, -7p13-p21.1, -7q32.3-q36.3, +8q22.2-q36.3, -9p21.3-p24.1, -11, -13, -14q11.2, -14q13.1-q32.33, -15q14-q26.3, +17q, -19q13.2-q13.43, -22q12.3-q13.33, -X

25	GIST	malignant	f/64	c-kit exon 11, PDGFRA ne	-1p36.21-p36.23, -6p25.3, -9, -14q, -19q13.43, -22q	ne
26	GIST	malignant	m/44	c-kit wt, PDGFRA wt	-1q31.2-q44, +8q23.2-q24.3, -14q	ne
27	GIST	malignant	m/54	c-kit wt, PDGFRA wt	-1p36.33-q22, -1q44, -2p25.3-q11.1, -4p15.33-p16.3, +5q13.3-q35.3, +5p12-q13.3, +6p12.3-q27, -6p12.3-p21.3, +9p24.1-p24.3, +10p11.21-p15.3, -13, -14q32.2-q32.33, -15q, -19, -21q22.11-q22.3, -22q	ne
28	GIST	malignant	f/74	ne	-9q22.31-q22.32, -9q31.2-q31.3, -14q, -22q	ne
29	GIST	malignant	m/72	ne	-1p36.1-p36.33, +4p15.2-q35.2, +7q11.23-q36.3, +9p13.3-p24.3, -11p15.5, -11q23.1-q25, -22q	-1p36.13-p36.33, -1p31.1, -1p13.3, -2, +4p16.3, +4q28.3, +5q31.3, +6p22.2, +6q21, +6q22.33, +7p22.1,+7q, +8q12.1, +8q23.1 , +8q24.21, +9p, -9q31.1, -11p14.2-p15.4, +11q13.1, +11q14.1, +11q14.2-q25, +12q13.3, +12q24.11, +12q24.23, -13, -15q, +17q11.2-q21.31, +17q25.1-q25.3, -18, -22q
30	GIST	malignant	f/39	ne	-1p, -10, -14q, -15q, +18p11.32-q23, -22q, -Xp22.32-p22.33	ne
31	GIST	malignant	m/32	ne	-1p31.3-p36.33, -2p25.3-q11.2, -4p15.2-p16.3, +4q21.22-q35.2, +6p12.3-q27, +6p12.3-p22.2, -8q24.3, +9p24.1-p24.3, -13q, -14q, -15q, +15q26.3, -19p13.3-q13.43, +21p11.2-q22.33, -22q,	ne
32	GIST	malignant	m/71	ne	-1p, +1q21.1-q32.1, +1q32.1-q44, -2p16.3-p24.1, +3, +4, +5, +6p22.1-p25.3, +6p12.1-p21.32, +7, +8, +9, -11, -13, -14q, -15q, -18, +16p13.3-q24.3, +17p13.3-q25.1, +19q13.1-q13.43, +20, +21	ne

33	GIST	malignant	f/42	ne	-1p35.1-p36.33, +2q37.3, -4p15.33-p16.3, -4q, +5, +8p21.3-q21.11, +8p21.3-p23.3, +8q23.2-q24.3, -9p13.2-q34.3, +12q13.2-q24.33, +13, +14q32.32-q32.33, -15q, +17q21.31, +17q25.1, +18q12.1-q23, +19q13.33, +20, -21p11.2-q21.1, -22q, -Xp22.32-p22.33	ne
34	GIST	malignant	m/54	c-kit exon 11, PDGFRA wt	-6p21.2-p21.3, -10p15.3-q11.21, -10q26.3, -14q, +X	ne
35	GIST	malignant	f/52	c-kit exon 11, PDGFRA wt	+3, +5, +6p21.3-p25.3, +6p12.2-q27, +8, +16, +20, -Xp22.31-p22.31	ne
wt= wild type ne = no experiment made - = copy number loss + = copy nunber gain						